DEFENCE S&T TECHNICAL BULLETIN

VOL. 9 NUM. 1 YEAR 2016 ISSN 1985-6571

CONTENTS

STRIDE

SCIENCE & TECHNOLOGY RESEARCH INSTITUTE FOR DEFENCE

AIMS AND SCOPE

The Defence S&T Technical Bulletin is the official technical bulletin of the Science & Technology Research Institute for Defence (STRIDE). The bulletin, which is indexed in, among others, Scopus, Index Corpenicus, ProQuest and EBSCO, contains manuscripts on research findings in various fields of defence science & technology. The primary purpose of this bulletin is to act as a channel for the publication of defence-based research work undertaken by researchers both within and outside the country.

WRITING FOR THE DEFENCE S&T TECHNICAL BULLETIN

Contributions to the bulletin should be based on original research in areas related to defence science & technology. All contributions should be in English.

PUBLICATION

The editors' decision with regard to publication of any item is final. A manuscript is accepted on the understanding that it is an original piece of work that has not been accepted for publication elsewhere.

PRESENTATION OF MANUSCRIPTS

The format of the manuscript is as follows:

a) Page size A4
b) MS Word format
c) Single space
d) Justified
e) In Times New Roman ,11-point font
f) Should not exceed 20 pages, including references
g) Texts in charts and tables should be in 10-point font.

Please e-mail the manuscript to:

1) Dr. Dinesh Sathyamoorthy (dinesh.sathyamoorthy@stride.gov.my)
2) Dr. Mahdi bin Che Isa (mahdi.cheisa@stride.gov.my)

The next edition of the bulletin (Vol. 9, Num 2) is expected to be published in November 2016. The due date for submissions is 7 September 2016. **It is strongly iterated that authors are solely responsible for taking the necessary steps to ensure that the submitted manuscripts do not contain confidential or sensitive material.**

The template of the manuscript is as follows:

TITLE OF MANUSCRIPT

Name(s) of author(s)

Affiliation(s)

Email:

ABSTRACT

Contents of abstract.

Keywords: *Keyword 1; keyword 2; keyword 3; keyword 4; keyword 5.*

1. TOPIC 1

Paragraph 1.

Paragraph 2.

1.1 Sub Topic 1

Paragraph 1.

Paragraph 2.

2. TOPIC 2

Paragraph 1.

Paragraph 2.

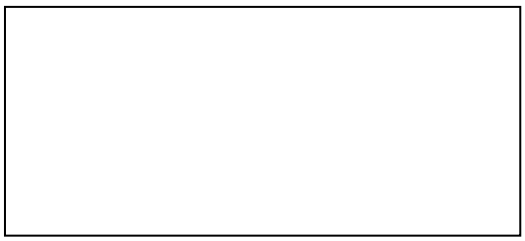

Figure 1: Title of figure.

Table 1: Title of table.

Content	**Content**	**Content**
Content	Content	Content
Content	Content	Content
Content	Content	Content

Equation 1 (1)
Equation 2 (2)

REFERENCES

Long lists of notes of bibliographical references are generally not required. The method of citing references in the text is 'name date' style, e.g. 'Hanis (1993) claimed that...', or '…including the lack of interoperability (Bohara *et al.*, 2003)'. End references should be in alphabetical order. The following reference style is to be adhered to:

Books

Serra, J. (1982). *Image Analysis and Mathematical Morphology*. Academic Press, London.

Book Chapters

Goodchild, M.F. & Quattrochi, D.A. (1997). Scale, multiscaling, remote sensing and GIS. *In* Quattrochi, D.A. & Goodchild, M.F. (Eds.), *Scale in Remote Sensing and GIS*. Lewis Publishers, Boca Raton, Florida, pp. 1-11.

Journals / Serials

Jang, B.K. & Chin, R.T. (1990). Analysis of thinning algorithms using mathematical morphology. *IEEE T. Pattern Anal.*, **12**: 541-550.

Online Sources

GTOPO30 (1996). *GTOPO30: Global 30 Arc Second Elevation Data Set*. Available online at: http://edcwww.cr.usgs.gov/landdaac/gtopo30/gtopo30.html (Last access date: 1 June 2009).

Unpublished Materials (e.g. theses, reports and documents)

Wood, J. (1996). *The Geomorphological Characterization of Digital Elevation Models*. PhD Thesis, Department of Geography, University of Leicester, Leicester.

ROBUST MULTIPLE CHANNEL SCANNING AND DETECTION OF LOW PROBABILITY OF INTERCEPT (LPI) COMMUNICATION SIGNALS

Ahmad Zuri Sha'ameri* & Abdulrahman Kanaa

Faculty of Electrical Engineering, Universiti Teknologi Malaysia (UTM), Malaysia

*Email: zuri@fke.utm.my

ABSTRACT

In this paper, multiple channel scanning and detection methods for low probability of intercept (LPI) signals in a multisignal environment are proposed. The short-time Fourier transform (STFT) and short-time Goertzel algorithm (STGA) are implemented to obtain the time-frequency (TF) representation. From the TF representation, different moving average (M_{avg}) lengths are used to detect the presence of the signal and their performance is verified. From the receiver operating characteristics (ROC), it is shown that the detection performance of STFT and STGA are close in terms of probability of detection (P_d) using the constant false alarm (CFAR) theorem at different probability of false alarms. STFT and STGA have P_d=0.9 using M_{avg}=32 at signal to noise ratio (SNR) of -15 dB and -14 dB respectively. However, STGA has computational complexity (CC) that is 10 times less than STFT. The instantaneous frequency (IF) estimated from the TF representation is able to identify the signals in a multisignal environment at SNR of 5 dB.

Keywords: *Low probability of intercept (LPI) signal; short-time Fourier transform (STFT); short-time Goertzel algorithm (STGA); probability of detection (P_d); computational complexity (CC).*

1. INTRODUCTION

The main components of electronic warfare (EW) - electronic support (ES), electronic attack (EA) and electronic protection (EP) – requires the scanning of the electromagnetic spectrum with maximum accuracy and speed. Typically, this is the primary function of the ES. However, both EA and ES in their secondary roles require the identification of emissions from both friendly and unfriendly sources before they can perform their primary roles. Difficulties occur to cover a large expanse of the electromagnetic spectrum and the analysis of signals in an extremely complex multisignal environment, whereby the received signals are highly diverse. They occupy a wide frequency band, and come from different sources with various modulation schemes and different levels of signal powers (Poisel, 2015). Thus, an ES system should be able to perform this task at high interception rate. Since it is passive, the ES system can detect the adversary with minimum probability of detection. Together with the presence of noise and interference, the bigger challenge is the detection and classification of low probability of intercept (LPI) signals (López-Risueño *et al*., 2005). Frequency hopping spread spectrum (FHSS) is a type of LPI signal when the carrier frequency is changed according to a random pattern only known to the communicating parties (Hassan *et al*., 2012). In addition, FHSS signal provides confidentiality since only the approved communicating parties with only perfect timing can readily demodulate the signal (Holmes, 2007). The resulting FHSS signal covers a large bandwidth such that detection is difficult by the ES system of the adversary. Furthermore, an EA system cannot use a spot jammer for a fixed frequency signal. Instead, a barrage jammer is needed where a higher jammer power is required (Adamy, 2015).

ES systems, also referred as EW systems, can be categorised as analog and digital systems (Tsui, 2004). Analog systems can be further classified into six general types: crystal video, superheterodyne,

instantaneous frequency measurement, channelised, compressive (microscan) and Bragg cell systems. The input signals are converted into video signals for further parameters estimation and classification through crystal detectors. Digital systems are developed due to the availability of high speed analog-to-digital converters and digital signal processing. After the signal is downconverted to the intermediate frequency, the signal is sampled to obtain its discrete-time representation for further processing. The main issues are the need to analyse signals at large bandwidth and the processing of signals close to real-time. Rather than to go to a fully digital system, the channelised receivers approach (Adamy, 2009) is used, which allows the simultaneous coverage of multiple adjacent frequency bands to include both fixed frequency signals and LPI signals such as FHSS signals. At each band, the downconverted signal at the intermediate frequency is sampled for further processing in discrete-time.

The objective of this paper is to describe the algorithms that allow accurate representation of the signal with reduced computational complexity (CC) to meet the requirements of an ES system. Due to the non-stationary nature of communication signals and multisignal environment, the time-frequency (TF) representation is required. The short-time Fourier transform (STFT) is used due to its low complexity. Furthermore, it does not introduce cross terms in a multisignal environment as opposed to quadratic TF representation (Boashash, 2003). However, the complexity of the TF representation can be further reduced. Unlike the discrete Fourier transform (DFT), the Goertzel algorithm performs the computation of a single DFT coefficient. Compared to the DFT, it is useful when only few frequency components are important and not the whole frequency spectrum. In this paper, a modified version of the Goertzel algorithm, known as short-time Goertzel algorithm (STGA), is introduced for non-stationary signals. The complexity of processing the signal in three dimension from the TF representation is simplified to two dimension by estimating the instantaneous frequency (IF) from the peak of the TF representation.

This paper is organised as follows: Section 2 describes an ES system, followed by Section 3 that defines the model, problem definition and frequency representation of a multisignal environment. The time-frequency analysis, detection method and instantaneous frequency (IF) estimation algorithm are discussed in Section 4, while the results and CC are presented in Section 5. Finally, the paper is concluded in Section 6.

2. ELECTRONIC SUPPORT (ES)

ES' primary function is to acquire and derive information or intelligence from the interception and identification of radiated electromagnetic energy, and also to determine the threat level, which forms the basis for further course of action (Adamy, 2009). The radiated electromagnetic energy could be information bearing signal such as communication signal or from non-information bearing signal such as radar signal. The use of ES depends whether it is for strategic or tactical use (Neri, 2006). For strategic use, the importance is on the gathering of intelligence over a long-term period with emphasis on the detailed signal parameters and accuracy. The tactical use of ES is to provide short term or close to real-time information that can be integrated as part of a weapon system.

The block diagram of an ES system is as shown in Figure 1 and covers the basic functions, including antenna system, emitter locating, parameter estimation, classification, and signal storage and retrieval (Sha'ameri & Boashash, 2015). Since the focus of this paper is on the detection of LPI communication signals, further details on the basic functions of an ES system to meet this requirement can be described as follows:

(1) Emitter locating – this is the main part of the system that determines the location of an airborne radar based on its emission. Among the basic methods used are angle of arrival estimation (AOA) (Poisel, 2012) and time-delay of arrival estimation (TDOA) (Sha'ameri *et*

al., 2015). With triangulation, AOA estimates from multiple sites to estimate the position of emitters.

(2) The frequency range for ES operations depends on the frequency band of interest. For tactical radios, the frequency range covers high frequency (HF), very high frequency (VHF) and ultra high frequency (UHF) bands from 3 MHz to 3 GHz. The monitoring of satellites and line of sight microwave links covers the microwave band at frequencies above 1 GHz. The use of specially designed ES systems based on the analog and digital systems is to meet the need to analyse LPI signals at large bandwidth and the processing of signals close to real-time.

(3) Once the signal is downconverted to the intermediate frequency or demodulated to video, the signal processing stage of the ES system first determines the frequency components within the captured bandwidth. The signal present at the detected frequency is then classified to determine the modulation type – whether its amplitude shift keying (ASK), frequency shift keying (FSK) and phase shift keying (PSK) - followed by the detailed analysis to estimate the signal parameters such the modulation frequencies, frequency deviation and phase.

(4) The parameters estimated at the signal processing stage are then used as input to a classifier (Tan *et al*., 2010). By matching the received parameters with the signal database, also referred to as the threat library, the classifier can determine if the received signal is a friendly, foe or unknown.

(5) The decision stage is when the operator decides on the next course of action based on the output from the classifier. Possible courses of action could be to investigate further, update the signal database, and activate countermeasures if the ES system is used at tactical level. At either tactical or strategic level, the signal could be decoded to extract the information content.

(6) The signal database contains all the possible information that describes the signal parameters classified from the received signal and other sources, electronic order of battle (EOB), and geographic information system (GIS).

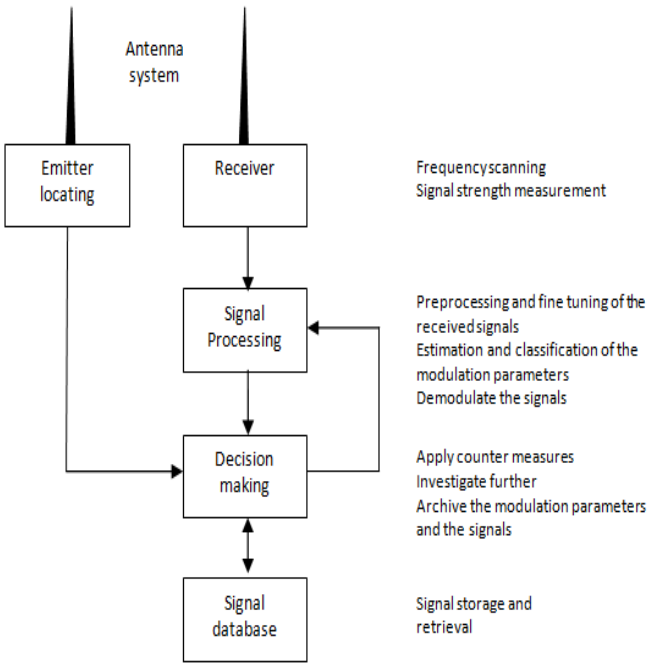

Figure 1: Block diagram of an ES system (Sha'ameri & Boashash, 2015).

The scope of this paper covers the signal processing component of the ES system and targets signal sources that come from fixed frequency signals and LPI signals specifically FHSS signals.

3. MULTISIGNAL ENVIRONMENT MODEL AND PROBLEM DEFINITION

The multisignal environment characteristics are first described in this section followed by the problem statement.

3.1 Multisignal Environment Model

The multisignal environment of interest consists of different communication signals. These signals occupy a set of M frequency channels for a given RF spectrum that covers a bandwidth of BW_{RF}. The received RF spectrum is downconverted to intermediate frequency by following the Nyquist sampling theorem at sampling frequency $f_s = 2BW_{RF.}$ Each channel is assumed to have an identical $BW_{ch} = BW_{RF}/M$. For this paper, the sampling frequency is assumed to be normalised at f_s =1 Hz and M =16 channels, which results in $BW_{ch} = f_s$ /32 Hz.

Each signal of the multisignal environment is randomly localised in time, whereby seven out of the 16 channels are occupied with signals of different modulation schemes: PSK, quadrature phase shift keying (QPSK) and FHSS, as described in Table 1. Each signal has a different start and end points. The FHSS signal occupies four channels and k represents the hop sequence .The hop duration is assumed to be 160 samples/hop and the modulation scheme is assumed to be PSK.

Table 1: Multisignal environment model. All signals have symbol duration of 160 samples.

Signal	Normalised Frequency (Hz)	Phase / Frequency Mapping	Start - End Points (Samples)
PSK1	3/32	$\phi_k(n) = \pi$ for s = 1 $\phi_k(n) = 0$ for s = 0	500 – 2,100
PSK2	14/32	$\phi_k(n) = \pi$ for s = 1 $\phi_k(n) = 0$ for s = 0	200- 2,000
QPSK	9/32	$\phi_k(n) = \pi/4$ for s = 11 $\phi_k(n) = 3\pi/4$ for s = 01 $\phi_k(n) = 5\pi/4$ for s = 00 $\phi_k(n) = 7\pi/4$ for s = 10	600 – 2,200
FHSS	BW= 6/32	$f_{h,k} = 6/32$ for k =1 $f_{h,k} = 8/32$ for $k = 2$ $f_{h,k} = 10/32$ for $k = 3$ $f_{h,k} = 12/32$ for $k = 4$	600-1,880

3.2 Problem Definition

The received signal can be defined as follows

$$y(n) = x(n) + v(n) \quad (1)$$

where $v(n)$ is additive white Gaussian noise (AWGN) with zero mean and variance σ_v^2.

AWGN is always present in communication signals, which leads to errors and consequently to significant degradation of the system performance. Furthermore, the signals of interest are assumed to be received in a non-cooperative environment with no prior knowledge of the signal characteristics. In digital communications, the detection is based on the maximum a posteriori criterion, where the priori probabilities of the transmitted symbols are equal. Since the prior probability of the received signal is unknown, the constant false alarm (CFAR) Neyman Pearson theorem is used, which relies a constant probability of false alarm P_{fa} and maximises the probability of detection P_d for a given P_{fa} (Barkat, 2005).

On the other hand, in conventional EW systems, frequency sweep represents a simple solution for multichannel scanning. This type of search system is called scanning superheterodyne system, where the frequency is linearly changed with time (Drentea, 2010). However, this method is not efficient for rapidly changing signals, such as FHSS signals, where the signal frequency changes faster than the sweeping speed. As a result, one or more frequency components of the signal will be missing. Moreover, the complexity increases proportionally with the number of scanned channels. Therefore, scanning multiple channels simultaneously requires a reduction in the computational complexity. Implementing a TF representation, such as STFT where multiple FFTs have to be calculated, leads to increased complexity. As a solution to avoid the multiple FFT calculation, multiple filters tuned at different frequencies of interest can be implemented. However, the filtering process is viewed as a convolution process with the complexity related to the number of filter coefficients. As a result, the increase in the number of filter coefficients will proportionally increase the complexity of the system. The approach is to use filters tuned to a centre frequency for STGA while for STFT, the window length is chosen to have the frequency bins located at the centre frequency of the signals of interest.

3.3 Frequency Representation of a Multisignal Environment

The power spectrum density (PSD) represents the distribution of frequency components of a given signal. It can be estimated either from the Fourier transform of the signal in time domain or using the Wiener-Khinchine theorem (Howard, 2004). It can be seen from the PSD of the signal that the time information of the signals is not represented. As a result, nonstationary LPI signals, such as FHSS, cannot be identified. As shown in Figure 2, the FHSS signal, with normalised frequencies: 0.187, 0.25, 0.3125 and 0.375 Hz, cannot be differentiated from the fixed frequency signals at normalised frequencies: 0.1, 0.2813 and 0.4375 Hz. The difference in the power shown in Figures 2(a) and 2(b) does not provide any indication of the presence a FHSS signal. By relying on the PSD, it will result in the misinterpretation on the actual signals present in the multisignal environment. Thus, a suitable representation is required that provides a joint representation in both time and frequency.

4. TF ANALYSIS, SIGNAL DETECTION AND IF ESTIMATION

In this section, the proposed TF representations are presented, the derivation of STGA is introduced followed by the moving average envelope detection method and finally, the IF estimation algorithm of a multisignal environment is explained.

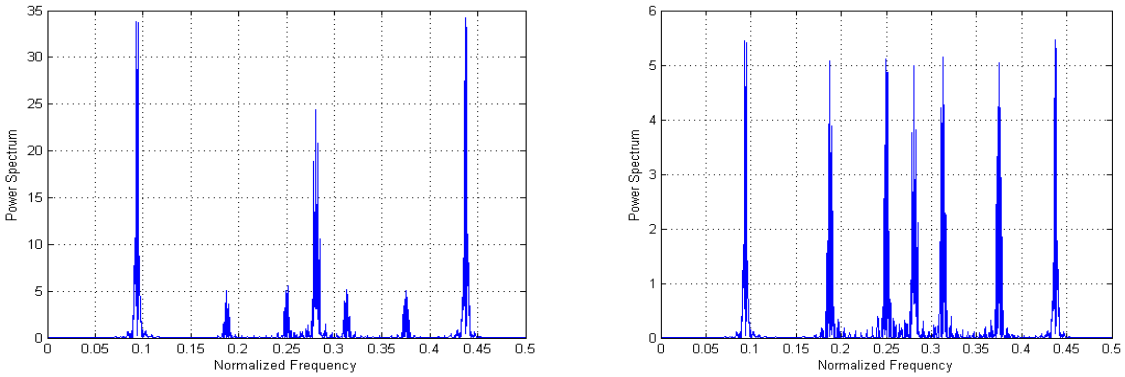

(a) Signals with different powers **(b) Signals with similar powers**

Figure 2: The PSD of a multisignal environment.

4.1 Short Time Fourier Transform (STFT*)*

STFT belongs to the class of linear time frequency distribution and is defined as (Hlawatsch & Boudreaux-Bartels, 1992; Boashash, 2003):

$$X(n,k) = \sum_{m=0}^{N-1} w(n-m)x(m)e^{-j\frac{2\pi km}{N_w}} \tag{2}$$

where N is the signal duration, $x(n)$ is the signal of interest and $w(n)$ is the window function of length N_w . The window function is defined such that:

$$\begin{aligned} w(n) &\neq 0 \quad for \quad 0 \le n \le N_w, N_w << N \\ &= 0 \quad elsewhere \end{aligned} \tag{3}$$

The definition of STFT in Equation 2 when interpreted as a filter bank representation (Quatieri, 2002) can be expressed as

$$X(n,k) = w(n) * \left(x(n)e^{-j\frac{2\pi kn}{N_w}} \right) \tag{4}$$

By factoring the complex exponential from Equation 4, the alternative representation is:

$$X(n,k) = e^{-j\frac{2\pi kn}{N_w}} \left[\left(w(n)e^{j\frac{2\pi kn}{N_w}} \right) * x(n) \right] \tag{5}$$

Thus, STFT is a series of N_w bandpass filters of duration N_w and centred at frequency k/N_w.

4.2 Short-Time Goertzel Algorithm (STGA)

The Goertzel algorithm is an alternative method to estimate the frequency representation. A reduction in complexity is possible compared to FFT if the signal occupies a limited number of frequencies(Engelberg, 2008; Sysel & Rajmic, 2012). This section describes STGA derived from DFT and the standard Goertzel algorithm.

The standard Goertzel algorithm considers the frequency representation for an N-length signal as the output of N band pass filters. For n time samples, Goertzel algorithm views the DFT as an output of a linear time invariant system:

$$\begin{aligned} y_k(n) &= \sum_{m=0}^{N-1} x(m) e^{j\frac{2\pi k(n-m)}{N}} \\ &= \sum_{m=-\infty}^{\infty} x(m) h_k(n-m) \qquad \text{for } 0 \le k \le N\text{-}1 \\ &= h_k(n) * x(n) \end{aligned} \tag{6}$$

where the system impulse response for the k^{th} frequency sample is:

$$h_k(n) = e^{j\frac{2\pi kn}{N}} u(n) \tag{7}$$

It can be seen from Equation 7 that $h_k(n)$ has an infinite impulse response due to the step function.

Since DFT is used in STFT as shown in Equation 2, it is desired to exploit the advantages of the Geortzel algorithm and use it in STFT. Unlike the system impulse response for the Goertzel algorithm in Equation 7, the system impulse response is limited to the window function length N_w. An equivalent effect can be achieved by introducing the attenuation coefficient (a) into Equation 7 and the resulting system impulse response is:

$$h_k(n) = a^n e^{j\frac{2\pi kn}{N_w}} u(n) \tag{8}$$

The selection of $|a|<1$ ensures the convergence of $h_k(n)$. The centre frequency is determined by the complex exponential in Equation 8 while the value of a is selected so that $h_k(n)$ has a bandwidth of $BW_{ch}=1/32$. This can be achieved by setting a=0.95. Figure 3 shows the frequency response of STGA for different values of a.

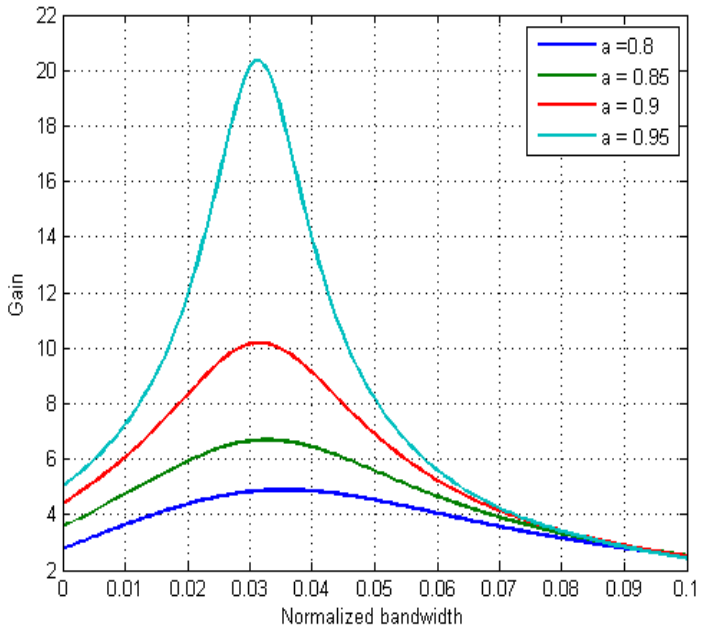

Figure 3: The frequency response of STGA.

4.3 Detection

Once the TF representation is obtained, the next step is to determine if the signal is present or not within a specific duration in time. For a given frequency k/N_w, the null hypothesis H_0 and alternate hypothesis H_1 are defined in the detection of signals as:

$$H_0 : y_k(n) = \frac{1}{M_{avg}} \sum_{m=0}^{M_{avg}} w(n-m) \left| v_{BW}(m) \right| \quad n = 1,2,.....N$$
$$H_1 : y_k(n) = \frac{1}{M_{avg}} \sum_{m=0}^{M_{avg}} w(n-m) \left| X(m,k) + v_{BW}(m) \right| \quad n = 1,2,.....N \tag{9}$$

where $X(n,k)$ is the TF representation of the signal, $v_{BW}(n)$ is a Gaussian noise observed within a bandwidth BW_{ch} , $w(n)$ is the averaging window, M_{avg} is the averaging window length, and N is the number of total captured samples. To simplify the notation, we assume that the signal and noise represented within a k^{th} channel as $X(n,k)=x$, $v_{BW}(\text{n})=v_{BW}$ and $y_k(\text{n})=y$.

Since the TF representation shown in Section 3 acts like the output of multiple bandpass filters, the noise received at each channel behaves like a narrowband Gaussian random process, where the consecutive noise samples are correlated. To ensure statistical independence, the noise samples are downsampled by f_s/BW_{ch} (Therrien, 1992). Since the detection is performed on the envelope of the output, the probability density functions (PDFs) of H_0 and H_1 are the joint PDFs of the M_{avg} of Rayleigh and Rician samples respectively. These PDFs have no closed form and unknown parameters, which is difficult to be estimated (Hu & Beaulieu, 2005; Nadarajah, 2008). To solve this problem, applying the central limit theorem (CLT) allows the sample average PDF to have approximately a Gaussian distribution (Bartoszynski & Niewiadomska-Bugaj, 2007). Thus, the distribution for H_0 is:

$$\rho_y(y \mid H_0) \sim \mathrm{N}\left(\sqrt{\frac{\pi}{2}} \sigma_{v_{BW}}, \left(\frac{4-\pi}{2} \right) \frac{\sigma_{v_{BW}}^2}{M_{avg}} \right) \tag{10}$$

where $\sigma_{v_{BW}}^2$ is bandpass noise power. Denoting Rayleigh standard deviation $\sigma_r = ((4-\pi)/2)\sigma_{v_{BW}}$, applying CLT based on averaging gives $\sigma_y = \sigma_r/\sqrt{M_{avg}}$ and Rayleigh mean $\mu_r = \sqrt{\pi/2}\sigma_{v_{BW}} = \bar{y}$. At the alternate hypothesis, Rician distribution at low SNR can be approximated as Rayleigh (Du & Swamy, 2010). Appendix A provides further details of the derivation. By applying the CLT, the distribution for H_1 is as follows:

$$\rho_y(y \mid H_1) \sim \mathrm{N}\left(\sqrt{\frac{\pi}{2}} \left(\sigma_x^2 + \sigma_{v_{BW}}^2 \right)^{1/2}, \left(\frac{4-\pi}{2} \right) \frac{(\sigma_x^2 + \sigma_{v_{BW}}^2)}{M_{avg}} \right) \tag{11}$$

where σ_x^2 is the received signal power. Similar to Eq. (10), to find the mean and variance of Equation 11, Rayleigh variance becomes $\sigma_r^2 = ((4-\pi)/2)\left(\sigma_x^2 + \sigma_{v_{BW}}^2\right)$.

Once the distributions of both the null and alternate hypotheses are acquired, the second step is to find the threshold γ based on the Neyman-Pearson theorem (MacDonough & Whalen, 1995), the probability of false alarm can be calculated as follows:

$$P_{fa} = P\left(H_1 \mid H_0\right) = \int_{\gamma}^{\infty} \rho_y(y \mid H_0) dy \tag{12}$$

Since the integration of a Gaussian function is complex, the *Q*- function is used and Equation 12 can be represented as:

$$P_{fa} = Q\left(\frac{\gamma - \overline{y}}{\sigma_y}\right) = Q\left(\frac{\gamma - \sqrt{\frac{\pi}{2}}\sigma_{v_{BW}}}{\sqrt{\frac{(4-\pi)\sigma^2_{v_{BW}}}{2M_{avg}}}}\right) \tag{13}$$

Solving Equation 13 for the detection threshold results in:

$$\gamma = \left(Q^{-1}(P_{fa})\sqrt{\frac{(4-\pi)}{2M_{avg}}} + \sqrt{\frac{\pi}{2}}\right)\sigma_{v_{BW}} \tag{14}$$

The probability of detection can be expressed as:

$$P_d = P\left(H_1 \mid H_1\right) = \int_{\gamma}^{\infty} \rho_y\left(y \mid H_1\right) dy \tag{15}$$

By substituting the detection threshold from Equation 14 into Equation 15, the probability of detection is:

$$P_d = Q\left(\frac{\gamma - \sqrt{\frac{\pi}{2}}(\sigma_x^2 + \sigma^2_{v_{BW}})^{1/2}}{\sqrt{\frac{(4-\pi)}{2}\frac{(\sigma_x^2 + \sigma^2_{v_{BW}})^{1/2}}{M_{avg}}}}\right) \tag{16}$$

The probability of missed detection where the signal is present but cannot be detected is defined as:

$$P_m = P(H_0|H_1) = 1\text{-}P_d \tag{17}$$

A trade-off is always present between P_{fa} and P_d, where by setting the P_{fa} to a high value increases P_d. However, high level of P_{fa} is not a favourable choice in many systems where false alarms can cause catastrophic results (Kay, 1998). The selection of P_{fa} is application dependent, for example, scanning in digital TV requires P_{fa} equals 0.1 with a high sensitivity receiver (Shellhammer, 2008). Recent work in (López-Benítez & Casadevall, 2012; Zhang *et al.*, 2013) shows that P_{fa} of 0.1 and 0.01 is used for energy detection method.

4.4 IF Estimation for a Mutlisignal Environment

The IF provides a more detailed view of the time-varying parameters in non-stationary signals. Moreover, to have a two-dimensional view of the signal of interest**,** the IFs of a multisignal environment are estimated from the peaks of the TF representation. The IF of a mono-component signal can be estimated from the peaks of the TF representation as follows (Boashash, 2003):

$$f_i(n) = \max_k [X(n,k)] \qquad 0 \le n \le N \tag{18}$$

where N is the length of the signal.

Since we have a multisignal environment, the received signal can be viewed as a sum of many signals. To estimate the IF of the multisignal environment, the following steps are implemented:

(1) Create an empty matrix to store the results, the size of the matrix will be equal to the TF representation matrix.

(2) Calculate the maximum energy of the TF representation.

(3) Set up a threshold at a level proportional to the maximum energy and set the time instant (t) to first time instant of TF representation (n_0).

(4) Find the maximum energy point of the TF representation at time instant n in Equation 18, the value should be above the predefined threshold.

(5) Store the value in the empty matrix, set the found TF representation value to zero and repeat Step 4 until all the channels at time instant n are scanned.

(6) Set time instant n to next time instant n+1 and go to Step 4.

(7) Repeat Steps 4-6 until no point above the threshold is found.

(8) Stop the search when the end of the TF representation matrix is reached.

At the end of Step 8, a matrix of values is obtained, the matrix has a dimension similar to the TF representation and the values represent the IF estimation of a multisignal environment.

5. RESULTS & DISCUSSION

In this section, we demonstrate the multisignal environment TF representations for both STFT and STGA algorithms. The performances of both algorithms are compared in terms of P_d at various SNRs and ROCs at different moving average lengths.

5.1 TF Representation

Figure 4 shows the TF representations for the received signals using STGA and STFT with no noise present. Even though both methods produce complex TF representations, for plotting purposes, the squared magnitude is shown. Without noise, it is easier to view the comparison between the TF representations. The result shows that seven channels from a total of 16 channels are occupied. For STFT, the window N_w is chosen at 32, which results in a frequency resolution of $f_s/32$. On the other hand, a equals to 0.95 gives a $BW_{ch} = f_s/32$ for STGA. In general, the TF representation describes the signals as defined in Table 1. Channels 4 and 15 are occupied with PSK1 and PSK2 at frequencies 3/32 and 14/32 respectively. The QPSK signal comes in Channel 10 at frequency 9/32 and FHSS signal covers four frequency channels at a BW of 6/32. It can be seen that PSK1 and PSK2 have different lengths of 1,600 and 1,800 with different start points at 500 and 200 respectively. Both the QPSK and FHSS signals have start point of 600 with signal durations of 1,600 and 1,280 respectively, and the FHSS signal hops at every 160 time samples. Therefore, both methods are able to clearly resolve the different types of signals jointly localised in both time and frequency.

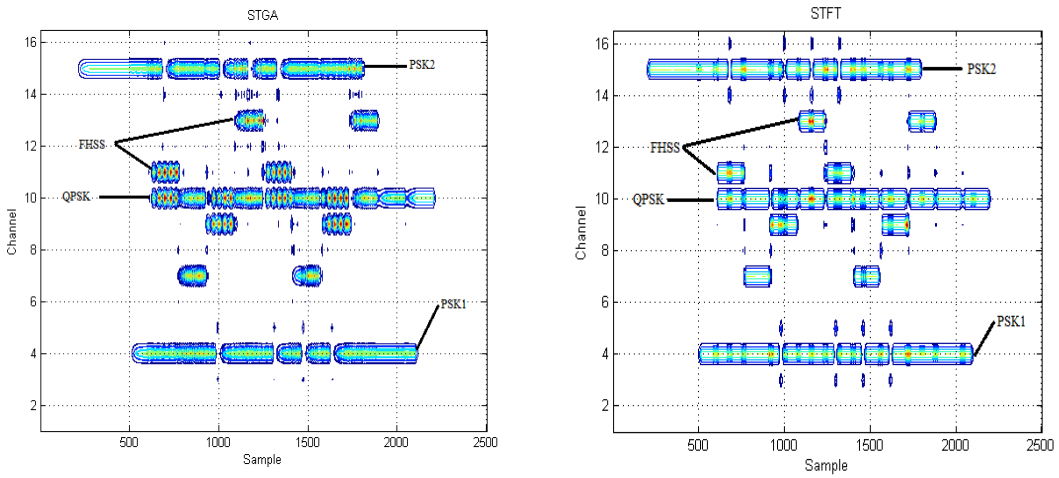

(a) STGA **(b) STFT**

Figure 4: TF representations of the multisignal environment showing different signals and their locations.

5.2 Receiver Performance (P_d *vs.* *SNR*)

Receiver detection performance illustrates the ability of the receiver to detect the signal of interest. It is measured, for both STFT and STGA, by evaluating P_d at SNR range from -35 to -5 dB at M_{avg}=32 samples. The theoretical results are calculated at various SNR ranges from Equation 16. This is done by varying σ_x^2 , which results in different P_d values. However, $\sigma_{v_{BW}}^2$ is assumed to be known, while the threshold γ is fixed and calculated from Equation 14 at a constant P_{fa}. On the other hand, the simulation results are obtained by implementing Monte Carlo simulation of 10^5 trials at each new value of σ_x^2 for the specified SNR.

The receiver detection performance is shown in Figure 5. It can be seen that to achieve P_d =0.9 at P_f=0.01, SNR of -14 and -15 dB is required for STGA and STFT respectively. However, at higher P_{fa}=0.1, SNR lower than 1 dB is needed for both STGA and STFT respectively. A comparison between simulation and theoretical results shows that the results are almost identical. Moreover, the results seen in Figure 5 shows that the performance of STFT is slightly better than STGA and the difference maximises at P_d of 0.9.

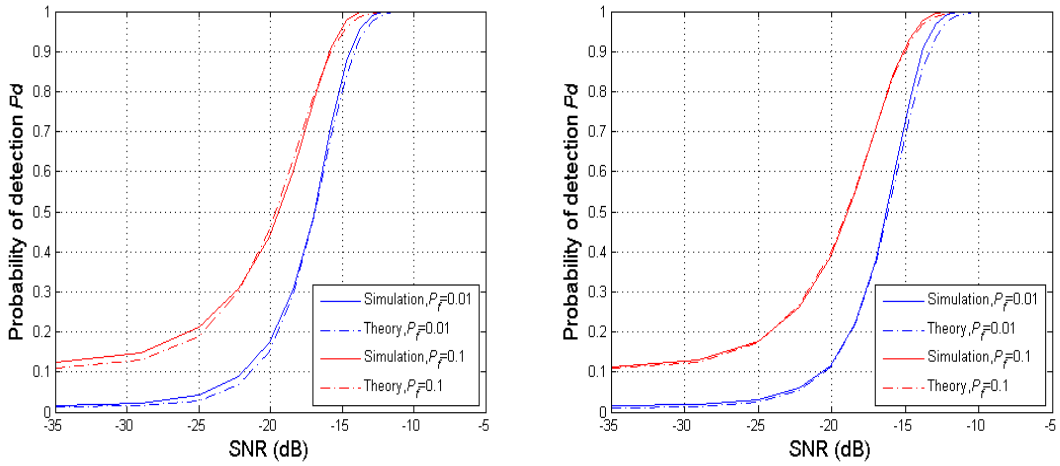

(a) STGA **(b) STFT**

Figure 5: Theoretical and simulation receiver detection performance at M_{avg}=32.

5.3 Receiver Operating Characteristics (ROC)

A better comparison can be obtained from the ROC, where the results show the relationship between P_d and P_f at a selected SNR. Assuming a known $\sigma^2_{v_{BW}}$ and a given P_{fa}, the threshold γ can be calculated from Equation 14. Moreover, the simulation results are obtained using Monte Carlo simulation at 10^5 trials at each new value of γ. The ROC can be measured at various SNRs. However, the SNR is chosen at -15 dB where P_d for both methods is around 0.9 as discussed in Section 5.2. It is shown in Figure 6 that theoretical ROC is slightly different from the simulation results. However, for P_f=0.1 at M_{avg}=32, P_d=0.8 and 0.9 is achievable for STGA and STFT respectively. Increasing M_{avg} to 64 gives better results at approximately P_d=0.95 for both TGA and STFT at the cost of a higher complexity as will be discussed in Section 5.5.

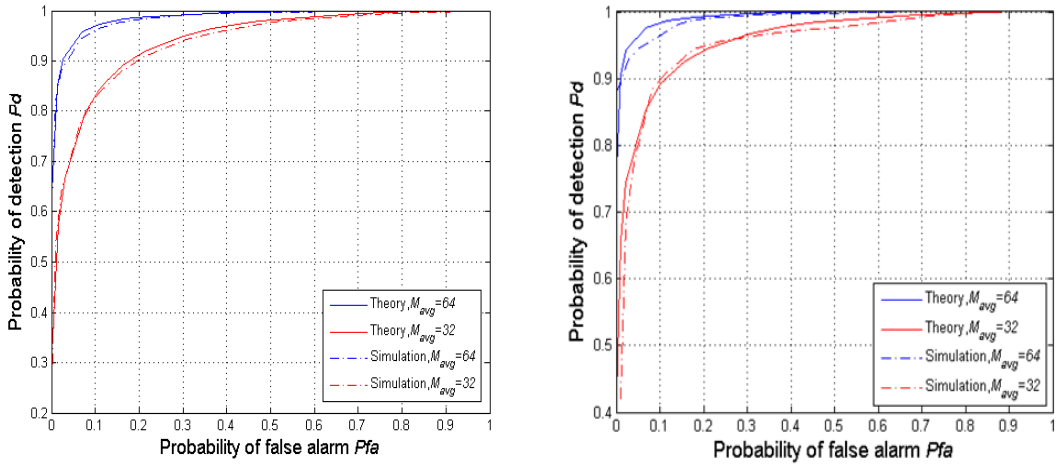

(a) STGA **(b) STFT**

Figure 6: ROC at SNR=-15 dB.

5.4 IF Estimation Results in a Multisignal Environment

In this section, the algorithm explained in Section 4.4 is implemented to estimate the IFs in the multisignal environment defined in Section 2.1. The IF estimation algorithm is evaluated at different levels of SNRs. The results in Figure 7 show that the performance declines as the SNR decreases. Figures 7 (a) and 7 (b) has the worst results because the signals are highly corrupted by AWGN. Although the TF representation in Figure 7 (a) does not clearly represent the signals of interest, the IF estimation in Figure 7 (b) can resolve most of the signal components. However, the artefacts are present because at certain time instances, the noise exceeds the threshold. The best result is obtained at SNR=10 dB in Figures 7 (e) and 7 (f), where both the TF representation and IF of each signal can be clearly estimated.

However, there is always a tradeoff between the threshold setting and the AWGN cancellation. Some parts of the signal cannot be detected if the threshold setting is too high. On the contrary, a low threshold results in letting in an addition amount of AWGN.

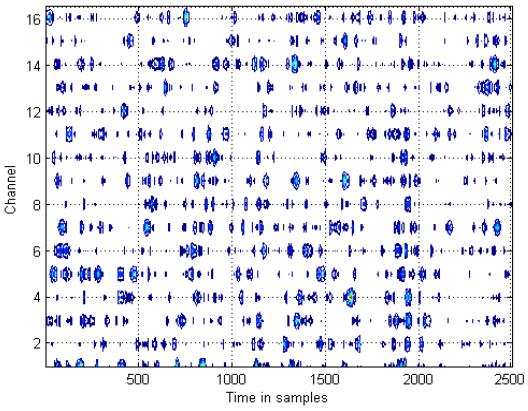

(a) TF representation, 0 dB

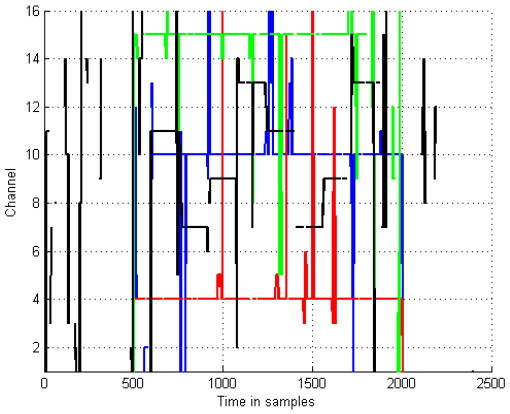

(b) IF estimation, 0 dB

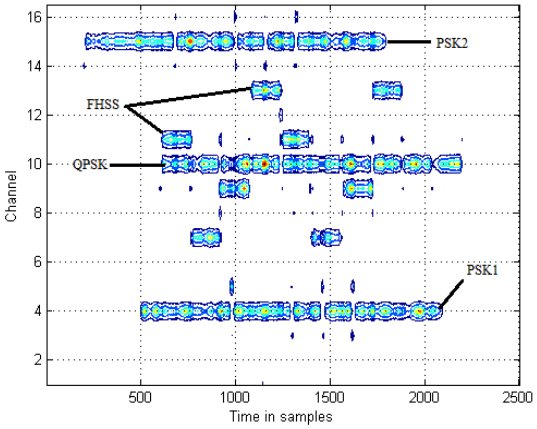

(c) TF representation, 5 dB

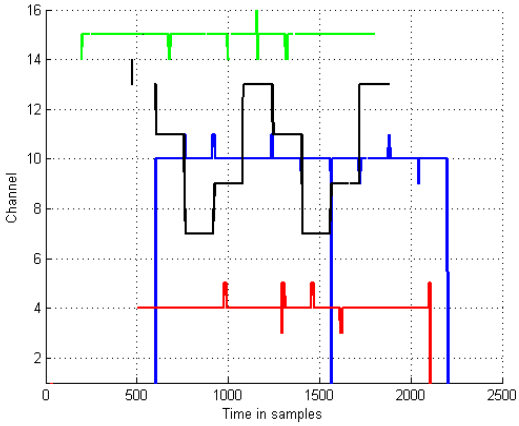

(d) IF estimation, 5 dB

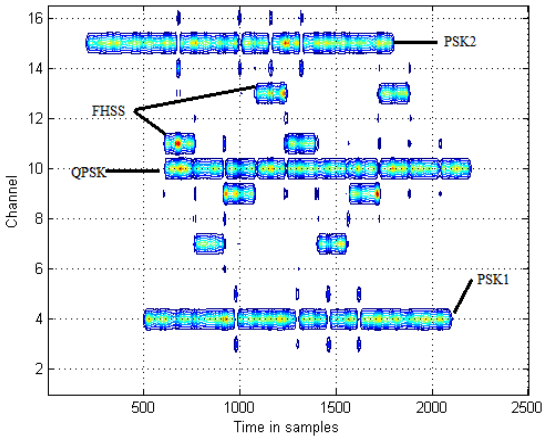

(e) TF representation, 10 dB

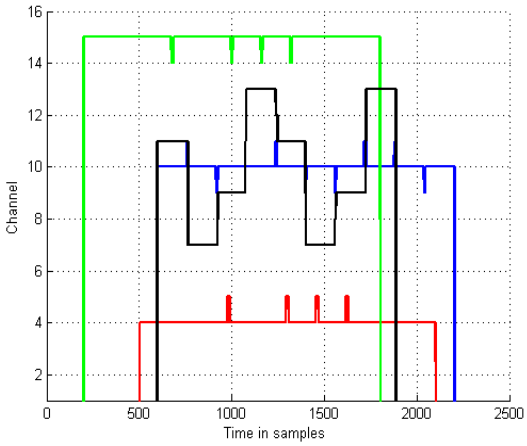

(f) IF estimation, 10 dB

Figure 7: TF representation and IF estimation in a multisignal environment at different SNRs.

5.5 Computational Complexity (CC)

The CC for scanning multiple channels is proportional the number of channels. Reducing the CC minimises the system latency and memory requirements. Since discrete time processing can be implemented on an embedded system, the signal and window lengths are defined in samples for both STFT and STGA. The same detection method used for TF representation is described in Section 6.

For STFT, the FFT algorithm is implemented over a window length N_w resulting in a CC of $N_w \log_2 N_w$ and it is performed over a signal duration of N. However, when complex values are taken into account, the CC becomes $6N_w \log_2 N_w$ (Sysel & Rajmic, 2012) . The CC for STFT based on Equation 2 is as follows

$$CC_{STFT} = N(6N_w log_2 N_w) \tag{19}$$

The implementation of STGA, shown in Equation 8, performs a bandpass filtering operation at every channel using a second order infinite impulse response (IIR) filter. The implementation of a second order IIR filter requires two real multiplication and one real addition for each channel at frequency k/N_w (Sysel & Rajmic, 2012). However, the CC doubles when the input value is complex. Consequently, the CC for STGA for a signal of length N is:

$$CC_{STGA} = 6NM \tag{20}$$

where $M=N_w/2$ represents the number of channels.

The detection method described in Section 4.3 has a moving average window $M_{avg,}$ which has a CC of:

$$CC_{detection} = (N/32)MM_{avg} \tag{21}$$

The multisignal environment IF estimation algorithm has been described in Section 4.4. It requires the finding of multiple maximum values along the frequency axis. The CC of finding the maximum value of a set of M values is $O(M)$ (Leiss, 2006). These values should exceed a certain preset threshold. As a result, the CC depends on the number of signal components of a multisignal environment presents at a given time, which may exceed a certain threshold value. Thus, the CC of the IF estimation can be described as:

$$CC_{IF} = mMN \tag{22}$$

where m is the number of signal components at a given time instant.

The total CC for the STFT can be calculated as follows:

$$CC_{STFT,total} = CC_{STFT} + CC_{detection} + CC_{IF} = N(6N_w log_2 N_w) + (N/32)MM_{avg} + mMN \tag{23}$$

Similary, the total CC for STGA is:

$$CC_{STGA,total} = CC_{STGA} + CC_{detection} + CC_{IF} = 6NM + (N/32)MM_{avg} + mMN \tag{24}$$

Since the detection and IF estimation algorithms are similar for both STFT and STGA, the CC comparison will be dependent on the TF representation calculations. From Equations 19 and 20, the CCs calculated for N=1,024 samples, M=16 channels and Nw=32 samples are 983,040 and 98,304 for STFT and STGA, respectively. In general, the CC for STGA is 10 times less than STFT. By having m=4, the total CCs calculated from Equations 23 and 24 are are 1,064,96 x10^6 and 2,785,28 x10^5 for STFT and STGA respectively.

6. CONCLUSION

In this paper, STFT and STGA are used to generate the TF representation and detect fixed frequency and FHSS signals in the multisignal environment. A moving average envelope detection method is introduced based on CFAR theorem and the threshold setting is selected to choose P_d and P_f. From the generated ROC, the signals can be successfully detected at P_f=0.1 and P_d=0.9 with SNR as low as -15 dB at M_{avg} =32. Further improvement in the signal detection can be achieved by increasing the M_{avg} length but at the expense of an increase in CC. Between STFT and STGA, both gave similar detection performances but the CC of STGA is 10 times lower than STFT. Therefore, it is more desirable to use STGA in a real multisignal environment. An algorithm is developed to estimate the IF of the multisignal environment from the TF representation. The IF estimated from the TF representation could successfully resolve the signals in the multisignal environment at SNR of 5 dB. From the estimated IF, further details on the signal parameters, such as frequencies, hopping rate and symbol rate, can be estimated.

APPENDIX A

Under the null hypothesis, the PDF is Rayleigh:

$$P(x \mid H_0) = \frac{x}{\sigma_{v_{BW}}} e^{\frac{-x^2}{2\sigma_{v_{BW}}}} \tag{A1}$$

The PDF the sum of M_{avg} independent samples:

$$P(x \mid H_0) = \prod_{i=0}^{M_{avg}-1} \frac{x_i}{\sigma_{v_{BW}}} e^{\frac{-x_i^2}{2\sigma_{v_{BW}}}} \tag{A2}$$

Having the average of M_{avg} independent samples and applying CLT for M_{avg}>>1, the PDF of null hypothesis becomes a Gaussian distribution as follow:

$$P(x \mid H_0) \sim \mathrm{N}\left(\sqrt{\frac{\pi}{2}}\sigma_{v_{BW}}, \left(\frac{4-\pi}{2}\right)\frac{\sigma_{v_{BW}}^2}{M_{avg}}\right) \tag{A3}$$

Under the alternative hypothesis, the PDF is Rician:

$$P(x \mid H_1) = \frac{x}{\sigma_{v_{BW}}^2} e^{\left(\frac{x^2+A^2}{2\sigma_{v_{BW}}^2}\right)} I_0\left(\frac{Ax}{\sigma_{v_{BW}}^2}\right) \tag{A4}$$

where A is the signal amplitude.

Denoting the signal variance $\sigma_x^2 = A^2/2$, at low SNR , Rician distribution can be approximated as Rayleigh distribution (Amini & Prince, 2013) where the peak of it is at $\sigma = \sqrt{\sigma_x^2 + \sigma_{v_{BW}}^2}$ approximately (Swanson, 2012). Taking the sum of M_{avg} independent samples, the PDF can be approximated as:

$$P(x \mid H_1) \sim \prod_{i=0}^{M_{avg}-1} \frac{x_i}{\sigma} e^{\frac{-x_i^2}{2\sigma}} \quad \text{(A5)}$$

As a result, applying CLT for M_{avg} >>1 of independent samples, the PDF of alternative hypothesis can be approximated as a Gaussian distribution:

$$P(x \mid H_1) \sim \mathrm{N}\left(\sqrt{\frac{\pi}{2}}\left(\sigma_x^2 + \sigma_{v_{BW}}^2\right)^{1/2}, \left(\frac{4-\pi}{2}\right)\frac{(\sigma_x^2 + \sigma_{v_{BW}}^2)}{M_{avg}}\right) \quad \text{(A6)}$$

ACKNOWLEDGEMENT

The authors would like to thank Universiti Teknologi Malaysia (UTM) under project Vot No. R.J130000.7924.4S118 and the Ministry of Science, Technology and Innovation (MOSTI), Malaysia for providing the resources for this research.

REFERENCES

Adamy, D. L. (2009). *EW 103: Tactical Battlefield Communications Electronic Warfare*. Artech House, Norwood, Massachusetts.

Adamy, D. L. (2015). *EW 104: Electronic Warfare Against a New Generation of Threats-EW100*. Artech House, Norwood, Massachusetts.

Amini, A.A. & Prince, J.L. (Eds.) (2013). *Measurement of Cardiac Deformations from MRI: Physical and Mathematical Models*. Springer, Berlin.

Barkat, M. (2005). *Signal Detection and Estimation*. Artech House, Norwood, Massachusetts.

Bartoszynski, R. & Niewiadomska-Bugaj, M. (2007). *Probability and Statistical Inference*. John Wiley & Sons, Hoboken, New Jersey.

Boashash, B. (2003). *Time Frequency Analysis*. Elsevier Science, Philadelphia, Pennsylvania.

Drentea, C. (2010). *Modern Communications Receiver Design and Technology*. Artech House, Norwood, Massachusetts.

Du, K. & Swamy, M. (2010). *Wireless Communication Systems*. Cambridge University Press Cambridge, UK.

Engelberg, S. (2008). *Digital Signal Processing: An Experimental Approach*. Springer, Berlin.

Hassan, A.A., Hershey, J.E. & Saulnier, G. (2012). *Perspectives in Spread Spectrum*. Springer, Berlin.

Hlawatsch, F., & Boudreaux-Bartels, G.F. (1992). Linear and quadratic time-frequency signal representations. *IEEE Signal Proc. Mag.,* **9**: 21-67.

Holmes, J.K. (2007). *Spread Spectrum Systems for GNSS and Wireless Communications*. Artech House, Norwood, Massachusetts.

Howard, R.M. (2004). *Principles of Random Signal Analysis and Low Noise Design: The Power Spectral Density and Its Applications*. John Wiley & Sons, Hoboken, New Jersey.

Hu, J. & Beaulieu, N.C. (2005). Accurate simple closed-form approximations to Rayleigh sum distributions and densities. *IEEE Commun. Lett.,* **9**: 109-111.

Kay, S.M. (1998). *Fundamentals of Statistical Signal Processing, Volume 2: Detection Theory*. Prentice Hall, Upper Saddle River, New Jersey.

Leiss, E.L. (2006). *A Programmer's Companion to Algorithm Analysis*. CRC Press, Boca Raton, Florida.

López-Benítez, M. & Casadevall, F. (2012). Improved energy detection spectrum sensing for cognitive radio. *IET Commun.,* **6**: 785-796.

López-Risueño, G., Grajal, J. & Sanz-Osorio, A. (2005). Digital channelized receiver based on time-frequency analysis for signal interception. *IEEE T. Aero. Elec. Syst., ,* **41**: 879-898.

MacDonough, R.N. & Whalen, A.D. (1995). *Detection of Signals in Noise*. Elsevier, Philadelphia, Pennsylvania.

Nadarajah, S. (2008). A review of results on sums of random variables. *Acta Appl. Math.,* **103**: 131-140.

Poisel, R.A. (2015). *Electronic Warfare Receivers and Receiving Systems*. Artech House, , Norwood, Massachusetts.

Quatieri, T.F. (2002). *Discrete-Time Speech Signal Processing: Principles and Practice*. Prentice Hall, Upper Saddle River, New Jersey.

Sha'ameri, A.Z. & Boashash, B. (2015). Time-frequency estimation of radio signal modulation parameters. *In* Boashash, B. (Ed), *Time Frequency Signal Analysis and Processing: A Comprehensive Reference (2nd Ed.).* Elsevier, Amsterdam, pp. 784-795

Shellhammer, S. J. (2008). Spectrum sensing in IEEE 802.22. *IAPR Wksp. Cognitive Info. Proc.*, pp. 9-10.

Swanson, D. C. (2012). *Signal Processing for Intelligent Sensor Systems with MATLAB,* Vol. 4. CRC Press, Boca Raton, Florida.

Sysel, P., & Rajmic, P. (2012). Goertzel algorithm generalized to non-integer multiples of fundamental frequency. *EURASIP J. Adv. Signal Proc.,* **Vol. 2012**: 1-8.

Therrien, C. W. (1992). *Discrete Random Signals and Statistical Signal Processing*: Prentice-Hall, , Upper Saddle River, New Jersey.

Tsui, J. (2004). *Digital Techniques for Wideband Receivers*. SciTech Publishing, Chennai, Tamil Nadu.

Zhang, S., Dong, X., Bao, Z., & Zhang, H. (2013). Adaptive spectrum sensing algorithm in cognitive ultra-wideband systems. *Wireless Personal Commun.,* **68**: 789-810.

STATISTICAL MODELLING FOR MISSING AND SPURIOUS PULSES IN PULSE REPETITION INTERVAL (PRI) ANALYSIS

Kamaruddin Abdul Ghani[1*], Kaharudin Dimyati[1], Ahmad Zuri Sha'ameri[2] & Nik Ghazali Nik Daud[1]

[1]Department of Electrical & Electronic Engineering, National Defence University of Malaysia (NDUM), Malaysia
[2]Faculty of Electrical Engineering, Universiti Teknologi Malaysia (UTM), Malaysia

*Email: kamaruddin@upnm.edu.my

ABSTRACT

Pulse repetition interval (PRI) analysis based on histogram method is widely used in electronic intelligence (ELINT) systems for emitter recognition. The identification of PRI modulation types using the statistical histogram method has faced inaccurate recognition due to error caused by missing and spurious pulses. In this study, the modelling for the statistical prediction of spurious and missing pulses is done to estimate their distributions density of occurrences that can be related to the robustness of the PRI analysis method. The statistical modelling is simulated using the histogram PRI analysis method and the proposed model is tested for its feasibility using Monte-Carlo simulation. The results obtained show that the proposed model can be used to estimate the presence of missing and spurious pulses, and can be used for testing of the robustness of PRI analysis methods.

Keywords: *Pulse repetition interval (PRI) modulation; histogram PRI analysis; spurious and missing pulses; Neymar-Pearson criterion; signal-to-noise-ratio (SNR).*

1. INTRODUCTION

Electronic intelligence (ELINT) analysis involves pulse train signal sorting. The purpose is to separate each pulse burst from signal flows of a large number of random overlapping pulses, and then selecting the useful deinterleaved signals (Jiang *et al*., 2013). The deinterleaving process is often carried out via clustering of multiple inter pulse parameters, such as time of arrival (TOA), pulse width (PW), angle of arrival (AOA), and radio frequency (RF) (Mahmoud *et al*., 2012). The analysis involves identifying the pulse repetition intervals (PRIs) in order to estimate the PRI modulation types, which is then used to identify the unique signatures of radar signals. The sorting and detection of a detected radar is then done by utilising the parameter library of the already known radars.

Most of the works on PRI analysis methods are based on statistical techniques with the histograms method (Mardia, 1989; Milojevic & Popovic, 1992; Guohua *et al*., 2009). It focuses on the sequence search algorithm based on the parameters of PRI. Intercepted radar pulse trains at ELINT receivers are corrupted with noise and clutter. Depending on the type of receiver, the level of noise differs from one receiver to another.

It is normal for spurious and missing pulses to appear in a single pulse train due to additive white Gaussian noise (AWGN). The effects of spurious and missing pulses can be catastrophic in PRI analysis especially if the number is high (Guobing & Yu, 2010). Missing and spurious pulses will introduce error in PRI measurements, which will lead to confusion in PRI modulation classification. A model to predict spurious and missing pulses is developed in this work that can be used as a platform to test PRI analysis methods. This work focuses on the Neyman-Pearson criterion where missing pulses can be predicted at given signal-to-noise-ratio (SNR) by setting the probability of spurious pulses. The prediction model may be used to test the robustness of new PRI analysis methods such as developed by Kamaruddin *et al*. (2015). For this work, the established histogram PRI analysis method is used.

2. SIGNAL MODEL AND PROBLEM DEFINITION

2.1 Signal Model

Every radar signal has a unique signature that can be used to identify the PRI modulation type, which is identified using PRI analysis. The most common PRI modulation types are constant, jittered and staggered (Figure 1) (Jingyao *et al*., 2009). Constant PRI means the interval between every two adjacent pulses is constant, while staggered PRI means the interval is a repetition of several fixed values. Jittered PRI means the interval is about a mean value but with a random jitter (*J*%) with maximum of 30% satisfying homogenous distribution (Noone, 1999). There are several variations of staggered PRI employed in radar such as 2-level, 3-level and so on depending on the number of repeating intervals (Montgomery, 1995).

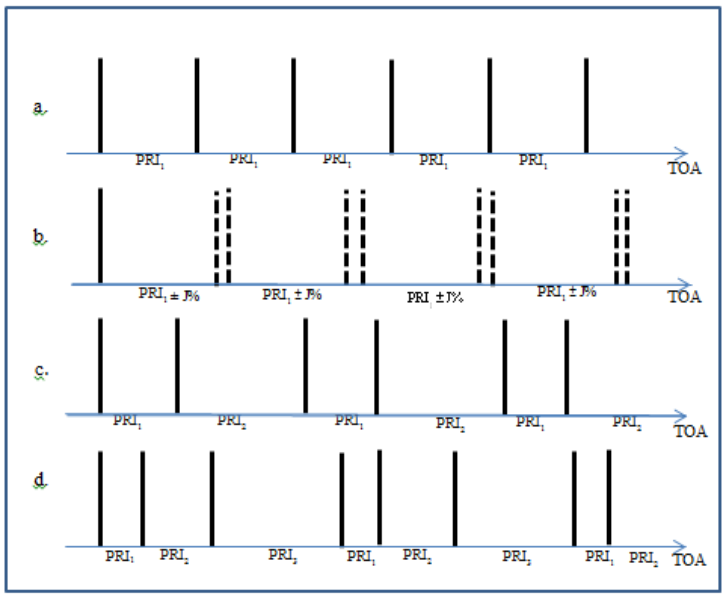

Figure 1: Common variations of PRI: (a) Constant (b) Jittered (c) 2-level staggered (d) 3-level staggered.

2.2 The Problem of Missing and Spurious Pulses

Normally, signals received at the receiver is corrupted with noise, especially AWGN. Noise and clutter contribute to error in PRI measurements by introducing spurious pulses and / or missing pulses. Besides noise, threshold level setting can also cause missing and/or spurious pulses (Figure 2). Spurious pulses occur when the threshold level is set too low, allowing noise to exceed it and be mistaken for a signal. On the other hand, if the threshold is set too high, weak signals might not exceed the threshold and would not be detected, resulting in missing pulses (Skolnik, 2001).

3. STATISTICAL MODEL FOR SPURIOUS AND MISSING PULSES

The detection of signal in noise is first described in this section followed by the statistical modelling for the spurious and missing pulses.

3.1 Detection of Signal in Noise

In a typical ELINT receiver, noise might exceed the threshold if it is set too low and be mistaken for a signal. This is called spurious pulse. The probability of this event happening is the probability of spurious pulses (P_{SP}). It represents the probability that noise will cross the threshold and be called a signal when only noise is present. On the other hand, if the threshold is set too high, while noise might not be large enough to cause spurious pulses, weak signals might not exceed the threshold and would not be detected. This is called missing pulse, and the probability of this event happening is probability of missing pulses (P_{MP}).

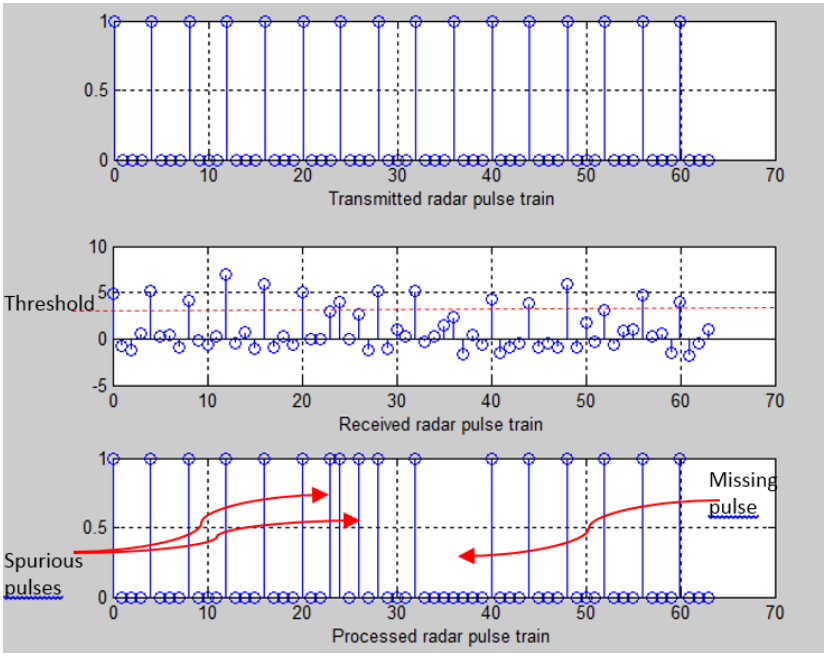

Figure 2: Simulated pulse train with missing and spurious pulses in an ELINT receiver.

Since noise is a random phenomenon, the detection of signals in the presence of noise is also a random phenomenon. The Gaussian partial density function (PDF) is important in detection theory since it describes many sources of noise. Since noise is a Gaussian PDF; the PDF for noise is given by:

$$Px(\mathrm{x}|H_0)= \frac{1}{\sqrt{2\pi\sigma}}\exp\left(-\frac{x^2}{2\sigma^2}\right) \quad (1)$$

where σ is the standard deviation and σ^2 is the variance. σ will determine the width of the Gaussian PDF of the noise or how wide the probability density is. The Gaussian distribution of noise for Equation 1 is as shown in Figure 3, where the peak centre of the distribution is $1/(\sqrt{2\pi\sigma})$. The signal too has Gaussian distribution where the PDF for signal is given by:

$$Px(x|H_1) = \frac{1}{\sqrt{2\pi\sigma}}\exp\left(-\frac{(x-A)^2}{2\sigma^2}\right) \quad (2)$$

where A is the mean value (signal gain) for the signal. For a radar system, the histogram analysis can be plotted for number of occurrence versus amplitude of the normalised histogram for both the noise and signal, such as in Figure 3. If the histogram is normalised with the total occurrence, it can be referred to that as the PDF. The centre distribution of the noise is denoted as '0'. In statistical testing it represents the null hypothesis (H_o). As for the signal, 1 is the signal gain and represents the alternate hypothesis (H_1).

If we set the threshold as shown in Figure 3, the blue shaded area is the P_{SP}. This is when only noise is present, which occurs whenever the noise is large enough to exceed the threshold and be mistaken as a signal. Another error occurs when a signal is present but is erroneously considered to be noise. This is the missing pulses, with the P_{MP} is shown in the pink shaded area.

In predicting the probabilities of spurious and missing pulses (P_{SP} and P_{MP} respectively), the statistical method with hypothesis testing is used involving the null and alternate hypotheses similar to radar systems. This work is based on radar false alarm and missed detection probabilities in a radar system. The probability of false alarm (P_{FA}) is represented by P_{SP} and the probability of missed detection (P_{MD}) is represented by P_{MP}. The probability density is dependent on the setting of the threshold voltage γ.

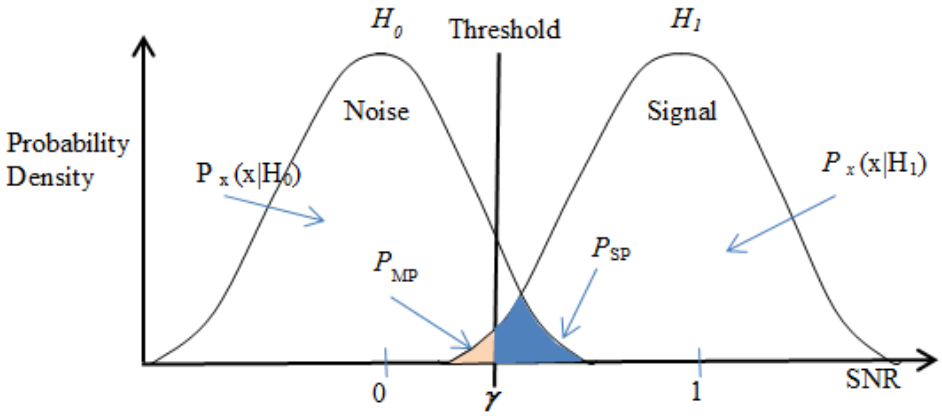

Figure 3: Probability density of spurious and missing pulses.

The choice of γ is critical as it will never reduce both probabilities. Reducing the threshold voltage will reduce the probability of missing pulses but in return will increase the probability of spurious pulses. On the other hand, if γ is increased to reduce the probability of spurious pulses, more missing pulses will occur. Both actions will not minimise the errors.

3.2 Neyman-Pearson Criterion

In digital communication, priori probability for receiving "0" or "1" is known where the probability is 50:50 (Sklar, 2001). However, in a radar system the priori probability is unknown. Therefore, this work is carried out by adopting the Neyman-Pearson criterion (Skolnik, 2001) to choose the correct density in an optimal manner. This is done by fixing one of the probabilities of error while minimising the other ones. The following procedure is required to calculate the PDF:

- Decide on P_{SP}
- From the P_{SP}, γ can be found
- Then decide on P_{MP}

According to the Neyman-Pearson theorem, for a fixed P_{FA}, for the likelihood ratio test for maximum detection, the detection rule is (Wickens, 2002):

$$L(x) = \frac{p(x|H_1)}{p(x|H_0)} > \gamma \tag{3}$$

with γ is the value for which

$$\int_{x:L(x)>\gamma} p(x|H_0)\, dx = P_{FA} \tag{4}$$

It is assumed that the work can tolerate 1% and 0.1% false alarms. Thus, the desired $P_{FA} = 10^{-3}$ and 10^{-2}, corresponding to $P_{SP} = 0.001$ and 0.01. By deciding on the P_{SP}, γ and P_{MP} can be determined using null and alternative hypotheses.

3.3 Null Hypothesis

Null hypothesis indicates the signal is not present but noise is. H_0 is used in setting the false alarm rate in a radar system. In this work, it relates to the spurious pulse rate determined based on the Neyman-Pearson criterion. Since the spurious pulse rate is fixed, it is independent of SNR. From PDF of the noise defined in Equation (1), P_{SP} can be determined by the threshold value as:

$$P_{SP} = \int_{\gamma}^{\infty} Px(x|H_0) \tag{5}$$

For P_{SP} = 0.001 and 0.01 (or similar to P_{FA} = 10^{-3} and 10^{-2}), the threshold values computed γ = 3.08 and 2.326 respectively.

3.4 Alternate Hypothesis

Alternate hypothesis indicates signal is present and is used to predict the probability of missed detection in a radar system. From alternate hypothesis, probability of detection, P_D can be calculated based on the PDF of signal defined in Equation (2):

$$P_D = \int_{\gamma}^{\infty} P_x(x|H_1)\, dx \tag{6}$$

Then probability of missing pulses can be computed as $P_{MP} = 1 - P_D$. Unlike spurious pulses, missing pulses is dependent on SNR.

3.5 Distribution of Spurious and Missing Pulses over an Observation Interval

The distribution for probability of spurious pulse is determined using Poisson distribution:

$$P_{SP} = e^{-N_p} \sum_{k=0}^{\infty} \frac{(N_p)^k}{k!} \delta(x-k) \tag{7}$$

for observation of N = 64 where $P_{SP}N < 1$. The distribution for P_{MP} is computed using binomial equation:

$$P_{MP} = \sum_{k=0}^{N} \binom{N}{k} p^k (1-p)^{N-k} (x-k) \tag{8}$$

for number of observation N=16 where $P_{MP}N > 1$, N_p is the mean and $N_p(1\text{-}p)$ is the variance. The SNR computed in this context refers to the particular pulse in the pulse train and not the average SNR of the train. The SNR for the signal can be computed as:

$$SNR_{dB} = 10 \log A^2 \tag{9}$$

The statistical model for missing and spurious pulses is applied to an established PRI analysis method i.e. histogram PRI analysis for classification of PRI modulation. For the whole model, as shown in Figure 4, with the generated AWGN, noise has zero mean and variance is 1.

4. RESULTS AND DISCUSSION

4.1 Histogram Analysis

The histogram method of PRI analysis is used to identify the modulation types of the PRI. Table 1 shows PRI classification results for constant, jittered and 2-level staggered signals. The histogram counts the number of occurrences of pulses. The most number of outcomes will determine the PRI modulation types.

4.2 Probability of Missing Pulse at Various SNRs

Five sequences of PRI are run through the system, which are constant sequence (C), jittered sequence (J), and three variations of staggered sequences; 2, 3 and 4-level staggered (represented by 2S, 3S and 4S respectively). A total of 64 pulses were used for all sequences in the simulations. A summary of the computed probability of missing pulse, P_{MP} for various SNRs is tabulated in Table 2 at different threshold levels.

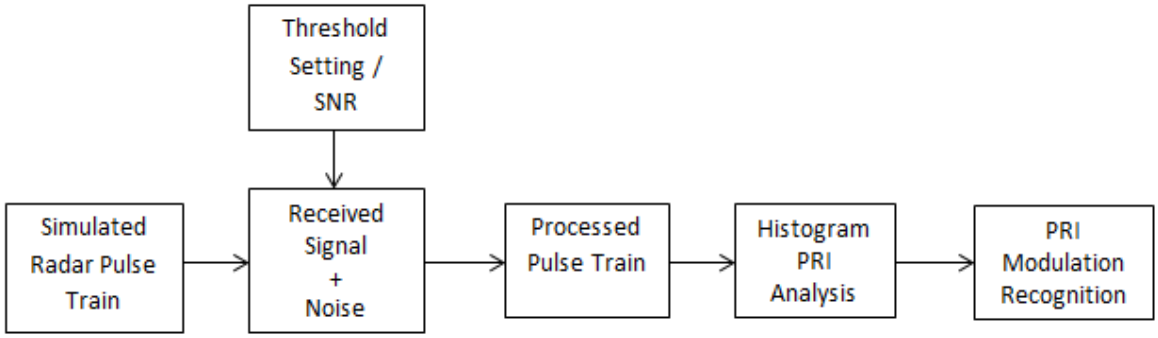

Figure 4: Block diagram for the proposed model.

Table 1: Samples of histogram results for selected PRIs.

PRI Type	Pulse Train Representations	Histogram Representation of PRI Types
Constant	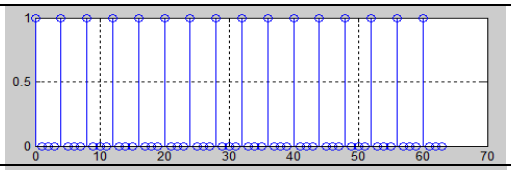	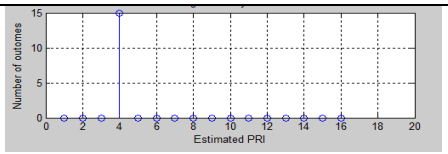
Jittered	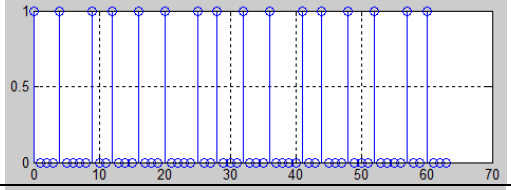	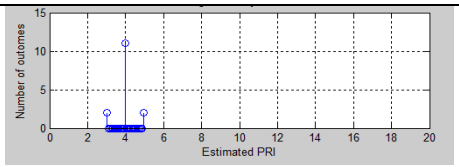
2-Level Staggered	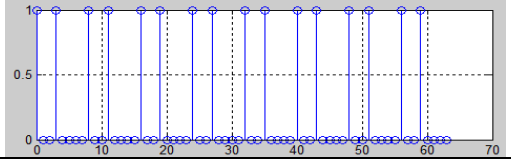	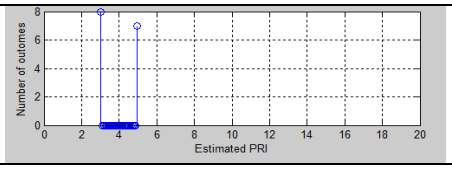

Table 2: Probability of missing pulses: (a) P_{MP} for $\gamma = 2.326$, $P_{SP} = 0.01$ (b) P_{MP} for $\gamma = 3.08$, $P_{SP} = 0.001$

SNR (dB)	P_{MP} for $\gamma = 2.326$, $P_{SP} = 0.01$ (a)	P_{MP} for $\gamma = 3.08$, $P_{SP} = 0.001$ (b)
6	0.6435	0.9813
7.9	0.4304	0.7728
9.5	0.296	0.4683
12	0.0472	0.1786
14	0.0038	0.0275
15.6	18×10^{-4}	1.2×10^{-4}
16.9	1.4797×10^{-6}	4.4375×10^{-5}
18	6.985×10^{-9}	4.335×10^{-7}

4.3 Distribution of Spurious Pulse in an Observed Pulse Train

Spurious pulses tend to have Poisson distribution. The probability of having spurious pulse at γ = 2.326 and P_{SP} = 0.01 is shown in the Poisson distribution of Figure 5. Probability of having no spurious pulse is 0.527 while probability of finding one spurious pulse is 0.335 and so on. In other words, 52.7% chances of getting no spurious pulse and 33.5% of getting one spurious pulse. The probability of getting at least one spurious pulse in the whole observation time is: P = 1 -0.527 = 0.473. Therefore, for every 64 observations, probability of getting at least one spurious pulse is 47.3%.

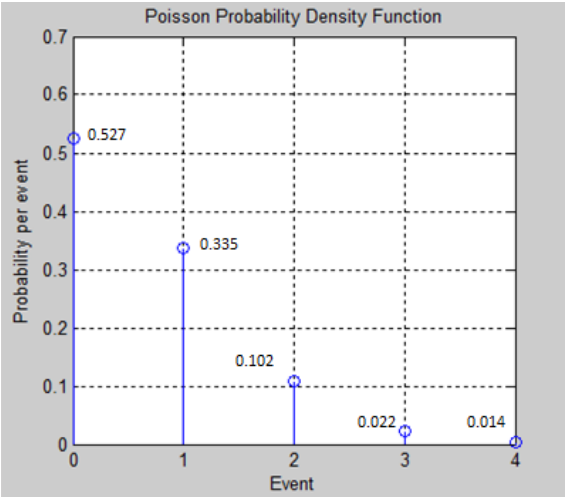

Figure 5: Distribution of spurious pulses at γ= 2.326, P_{SP} = 0.01.

Figure 6 shows the probability of spurious pulses at higher threshold, γ = 3.08 or P_{SP} = 0.001. The probability of having no spurious pulse in the observation is 0.93, while the probability of having one spurious pulse is 0.07. There is no probability of getting two or more spurious pulses at this threshold level as the higher threshold reduces the chances of having spurious pulses. Probability of getting at least one spurious pulse at this threshold is: P = 1 – 0.93 = 0.07 Therefore, for every 64 observations, the probability of getting at least one spurious pulse at threshold γ = 3.08 is 7%. The chances of getting at least one spurious pulse at γ = 3.08 is lower than γ = 2.326. Thus, increasing the threshold will reduce the probability of getting spurious pulses, regardless of SNR.

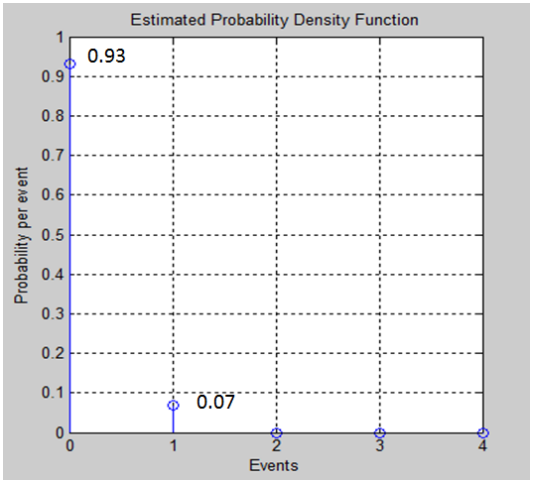

Figure 6: Distribution of spurious pulses at γ= 3.08, P_{SP} = 0.001.

4.4 Distribution of Missing Pulses in an Observed Pulse Train

Missing pulses have a binomial distribution. Figure 7 shows the binomial distribution for probability of missing pulses at threshold, $\gamma = 2.326$ with SNR = 6 dB for constant PRI. The mean is 11 with probability of missing pulse, $P_{MP} = 0.20$ which indicates there is a 20% chance of missing pulses for the observation period of the pulse train. In other words, for 100 loops of Monte-Carlo simulation run for the proposed model, there is a probability of getting 80% correct classifications.

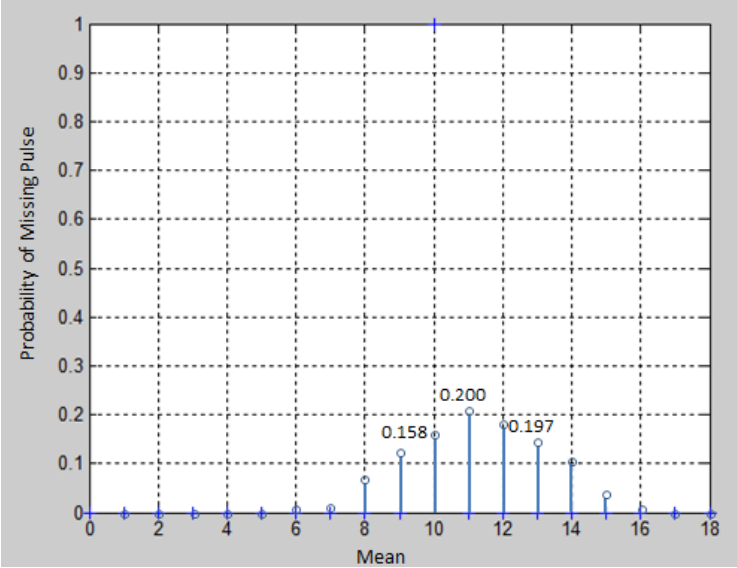

Figure 7: Probability of missing pulses at $\gamma = 2.326$, $P_{SP} = 0.01$.

For the higher threshold, $\gamma = 3.08$, the probability distribution of missing pulses is shown in Figure 8. Higher probability of missing pulse is observed at higher threshold with 79.3% chance of getting missing pulses with mean value of 16. This satisfies the theory explained in Figure 3.

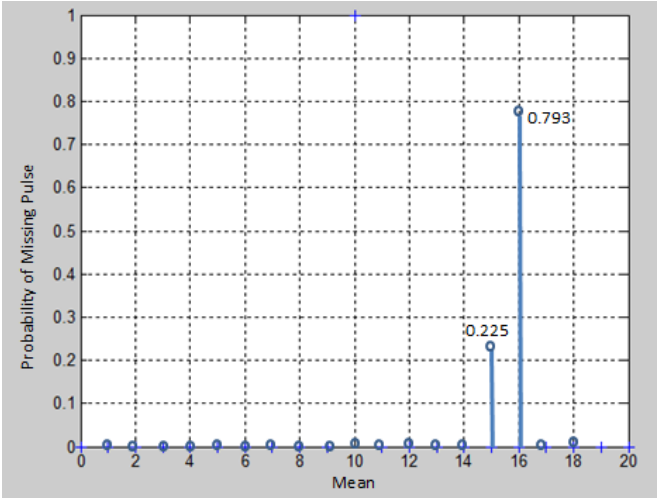

Figure 8: Probability of missing pulses at $\gamma = 3.08$, $P_{SP} = 0.001$.

4.5 PRI Classification Results

To verify the performance, Monte-Carlo simulation is performed by running the model for 100 sequences of pulse trains to determine the probability of correct classification (P_{cc}) at a given SNR range from 0 to 18 dB. The confusion matrix also known as the error matrix or contingency table (Stephen, 1997), provides a better insight of pulse train that are misclassified. Entries along the diagonals signify correct classification, while the non-diagonals entries signify otherwise (Wickens, 2002; Ahmad & Sha'ameri, 2015). Two confusion matrices are presented for lower SNR (6 dB) and higher SNR (14 dB) in Table 3.

Table 3: Confusion matrices for: (a) SNR=6 dB (b) SNR = 14 dB.

	C	*J*	*2S*	*3S*	*4S*
C	61	38	1	0	0
J	0	50	50	0	0
2S	0	27	71	2	0
3S	0	35	0	61	4
4S	0	51	0	0	49

(a)

	C	*J*	*2S*	*3S*	*4S*
C	79	20	1	0	0
J	0	74	21	5	0
2S	0	22	75	1	2
3S	0	11	0	82	7
4S	0	21	0	0	79

(b)

For constant PRI at SNR = 6 dB, out of 100 samples, the system predicted that 61 are constant, 38 are jittered and one is 2-level staggered. For jittered signals, 50 are predicted as jittered while 50 as 2-level staggered. As shown in Table 3(a), the probability of correct of classification (P_{cc}) at SNR = 6dB is between 50 - 70%.

At SNR = 14 dB, as shown in Table 3(b), the classification accuracy is 79% for constant, 74% for jittered, and more than 75% for all staggered signals. All the PRIs have correct classification of around 80%, which satisfies the distribution of missing pulses discussed in Section 4.4. Thus, at higher SNR, the percentage of correct classification is higher than lower SNR.

The results obtained indicate that percentage of correct classification increases as SNR increases. This is as the probability of missing pulses for PRI modulation is directly related to SNR. As SNR increases, the confusion decreases. Raising the threshold reduces spurious pulses and increases the SNR required for a specified probability of detection.

5. CONCLUSION

In this study, the prediction for probability density of spurious and missing pulses was modelled. Using Neyman-Pearson criterion, the presence of missing pulses was able to be predicted given SNR by setting the probability of spurious pulses. Probability of spurious pulses is independent of SNR, increasing the threshold will reduce the probability of getting spurious pulses, regardless of SNR. On the other hand, probability of missing pulses is dependent on SNR with higher SNR leads to increasing in probability of correct classification. The proposed model can be used to measure the robustness of PRI analysis tools for missing and spurious pulses.

ACKNOWLEDGEMENT

This research work is supported by the FRGS Grant FRGS/2/2014/TK03/UPNM/02/3.

REFERENCES

Ahmad, A. A. & Sha'ameri, A. Z. (2015). Classification of airborne radar signals based on pulse feature estimation using time-frequency analysis. *Defence S&T Tech. Bull.* **8:**, 103-120.

Guobing, H. & Yu, L. (2010). An efficient method of pulse repetition interval modulation recognition. *Int. Conf. Comm. and Mobile Comput*., 287-291.

Guohua, G., Yan, M., Jun, H. & Xu, Q. (2009). An improved algorithm of PRI transform. *Global Congress Int. Sys*., pp. 145-149.

Jiang, Y., Haiqing, J. & Zhenxing, L. (2013). Design and implementation on sorting and tracking processor for radar signal based on DSP. *World Congress Soft. Eng*., 145-149.

Jingyao, L., Huadong, M. & Xiqin, W (2009). A new pulse deinterleaving algorithm based on multiple hypothesis tracking, *Int. Radar Conf*., pp. 1-4.

Kamaruddin, A. G., Ahmad Zuri, S. & Kaharudin, D. (2015). Development of a pulse repetition interval (PRI) modulation template using Walsh-Hadamard Transform (WHT). *Defence S&T Tech. Bull.,* **8**: 42-50.

Mahmoud, K., Mansour, P.A. & Farouhar, F (2012). A new method for detection of complex pulse repetition interval modulations. *Proc. ICSP*, Vol. 3, pp. 1705-1709.

Mardia, H. K. (1989). New techniques for the deinterleaving of repetitive sequences. *Proc. RSP*, Vol.6, pp. 149-154.

Milojevic, D. J. & Popovic, B. M. (1992). Improved algorithm for the deinterleaving of radar pulses. *Proc. RSP, Vol.13, pp.* 98-104.

Montgomery, H.T. (1995). *SARIE Groundbased ELINT System.* Training Manual, Sysdel CC/BK, Pretoria.

Noone, G.P. (1999). A neural approach to automatic pulse repetition interval modulation recognition. *Proc. IDC, pp. 213-218.*

Sklar, B. (2001). *Digital Communications: Fundamentals and Applications.* Prentice, New York.

Skolnik, M. (2001). *Introduction to Radar Systems*. McGraw-Hill, New York.

Stephen, V. S. (1997). Selecting and interpreting measures of thematic classification accuracy. *Remote Sensing Env.,* **62**: 77-89.

Wickens, T. D. (2002). *Elementary Signal Detection Theory*. Oxford University Press, New York.

APPLICATION OF SELF-ORGANIZING MAP (SOM) FOR CLUSTERING OF LANDFORMS IN THE WEST OF THE FARS PROVINCE, IRAN

Marzieh Mokarram[1*] & Dinesh Sathyamoorthy[2]

[1]Department of Range and Watershed Management, College of Agriculture and Natural Resources of Darab, Shiraz University, Iran.
[2]Science & Technology Research Institute for Defence (STRIDE), Ministry of Defence, Malaysia

[*]Email: m.mokarram@shirazu.ac.ir

ABSTRACT

The aim of this study is to cluster landforms in the west of the Fars province, Iran using self-organizing maps (SOM). According to qualitative data, the clustering tendencies of landforms are investigated using six morphometric parameters, which are slope, profile, plan, elevation, curvature and aspect. First, topographic position index (TPI) is used to prepare the landform classification map. The results of SOM show that there are five classes for landform classification in the study area. Cluster 5 corresponds to high slope, high elevation but with different of concavity and convexity that consist of ridge landforms, while Cluster 3 corresponds to flat areas, possibly plantation areas, in medium elevation and almost flat terrain. Clusters 1, 2 and 4 correspond to channels with different slope conditions.

Keywords: *Clustering; landforms; morphometric parameters; topographic position index (TPI); U-matrix*.

1. INTRODUCTION

Landforms are the result of geomorphologic processes that occur on the earth's surface. The term landform is used for morphometrically homogeneous land-surface regions due to the effects of common geological and geomorphological processes (Crevenna *et al*., 2005). As this concept of landforms is an idealized one, it then follows that the closer the studied landform conforms to its definition, the greater the accuracy of the obtained model. A sub-discipline of geomorphology is geomorphometry, which provides quantitative and qualitative description and measurement of landforms (Pike & Dikau, 1995; Dehn *et al*. 2001; Pike 2002; Crevenna *et al*., 2005), and is based on the analysis of variations in elevation as a function of distance. A basic underlying principle of geomorphometry is digital elevation models (DEMs). A number of studies have employed DEMs for the automated mapping of landforms (MacMillan *et al*., 2000; Burrough *et al*., 2000, Meybeck *et al*., 2001, Schmidt & Hewitt, 2004; Saadat *et al*., 2008). Derivation of landforms can be carried out using various approaches, including classification of terrain parameters (Dikau 1989; Dikau *et al*., 1995), filter techniques (Sulebak *et al*., 1997), cluster analysis (Etzelmuller & Sulebak, 2000) and multivariate statistics (Adediran *et al*., 2004). A common focus of the study of landforms is to consider them as formed by small and simple elements which are topologically and structurally related. A more complete description of landform may be achieved by using complex terrain parameters calculated from simple ones, e.g., the topographic wetness index (Moore & Nieber, 1989), stream power index (Moore *et al*., 1993a), aggradation and degradation indices (Moore *et al*., 1993b), thresholds (Dikau, 1989), automated classification using object-based image analysis (Dragut & Blaschke, 2006) multivariate descriptive statistics (Evans,1979; Dikau,1989), double ternary diagram classification (Crevenna *et al*., 2005), discriminant analysis (Giles, 1998), fuzzy logic and

unsupervised classification (Adediran *et al*., 2004; Burrough *et al*., 2000; Mokarram *et al*., 2014) and neural networks (Ehsani & Quiel, 2008).

Self-organizing map (SOM) is an unsupervised and non-parametric artificial neural network (ANN) algorithm that clusters high dimensional input vectors into a low dimensional (usually two-dimensional) output map that preserves the topology of the input data (Ehsani & Quiel, 2008). Preserving topology means that the SOM map preserves the relations between the input neighboring points in the output space (Kohonen, 2001). Hosokawat & Hoshit (2001) used SOM to generate a damage distribution map in Kobe city, Japan that corresponds with the actual damage recorded following the 1995 earthquake. Ehsani & Quiel (2008) employed SOM and Shuttle Radar Topography Mission (SRTM) data to characterize yardangs in the Lut desert, Iran. The results demonstrate that SOM is a very efficient tool for analyzing aeolian landforms in hyper-arid environments that provides very useful information for terrain feature analysis in remote regions. Ferentinou & Sakellariou (2010) applied SOM in order to rate slope stability controlling variables in natural slopes, while Ferentinou *et al*. (2010) used SOM to classify marine sediments. Mokarram *et al*. (2014) used SOM to study the relationships between geomorphological features of alluvial fans and their drainage basins. The results of the analysis showed that several morphologically different fan types were recognized based on their geomorphological characteristics in the study area.

The west of Fars, Iran has the highest points in the Fasa city, with a rich wildlife preserve, known as Kharmankooh, which is a hunting prohibited region. The area has a variety of landforms that is suitable for the wildlife. As different animals live in different landforms, clustering of landforms can be used to predict the type of wildlife in the study area. To this end, the aim of this study is to cluster the landforms using SOM based on morphometric characteristics.

2. MATERIAL AND METHODS

2.1 Study Area

The study area is located in the west of the Fars province, southwest Iran, which is shown in Figure 1. It is located between 29° 00′ to 29° 25′ N and 53° 19′ to 53° 54′ E (Figure 1). Six morphometric parameters were analyzed; slope, profile, plan, elevation, curvature and aspect (Figure 2 and Table 1).

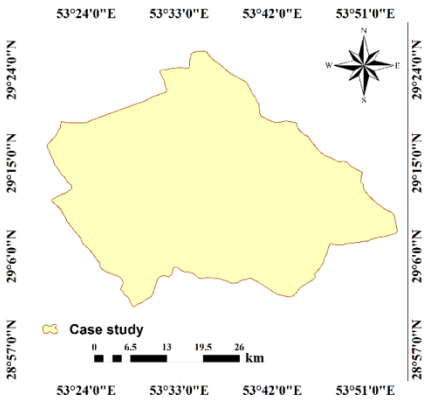

Figure 1: Location of the study area.

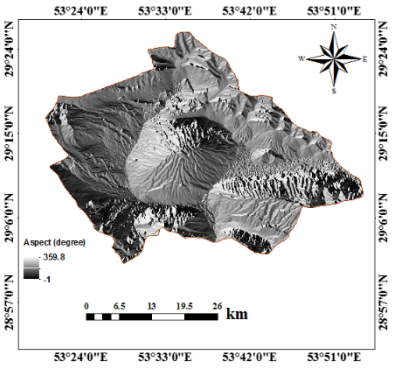

Aspect

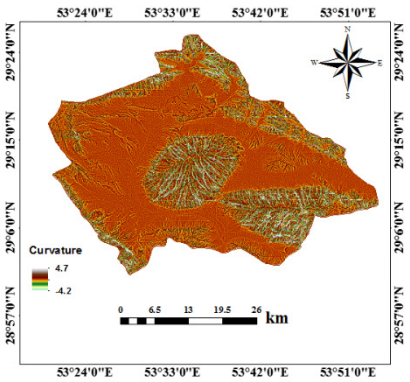

Curvature

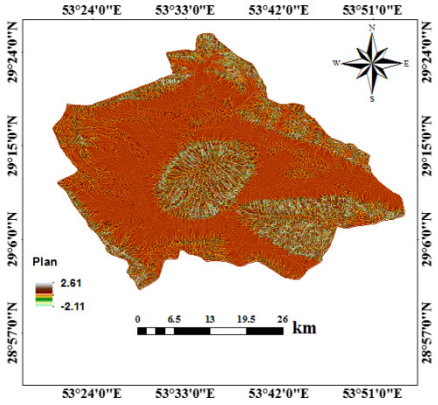

Plan

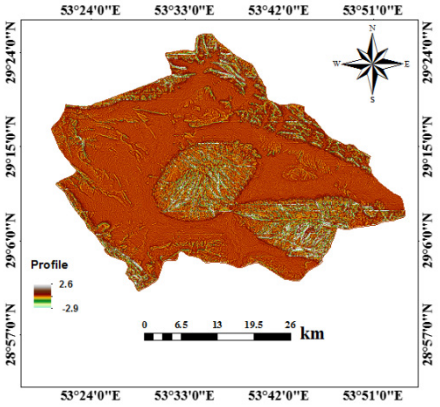

Profile

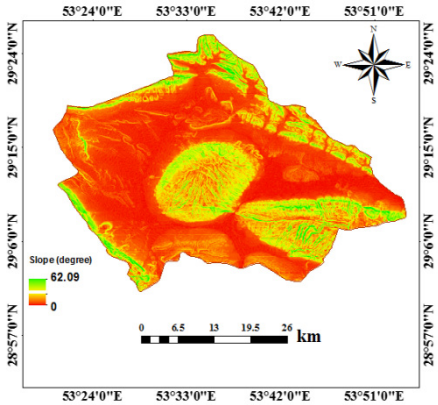

Slope

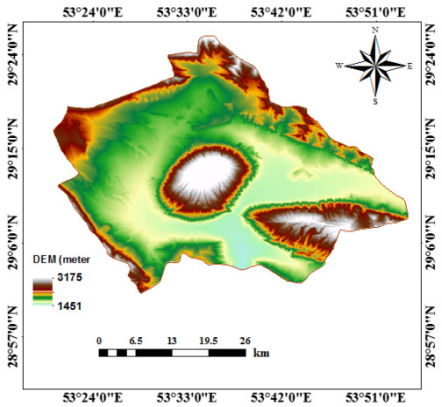

Elevation

Figure 2: Morphometric parameters of the study area.

Table 1: Morphometric parameters measured for the determination of landform classification.

Parameter	Min	Max	Average	STDVE
Slope (°)	0.38	42.12	9.94	12.11
Profile (1/m)	-0.40	0.44	0.01	0.14
Plan (1/m)	-0.48	0.66	0.01	0.20
Elevation (m)	1484.00	2805.00	1898.58	345.93
Curvature (1/m)	-0.48	0.98	0.01	0.26
Aspect (°)	7.70	358.15	169.42	111.06

2.2 Landform Classification Using Topographic Position Index (TPI)

TPI (Weiss, 2001) compared the elevation of each cell in a DEM to the mean elevation of a specified neighborhood around that cell. Positive TPI values represent locations that are higher than the average of their surroundings, as defined by the neighborhood (ridges). On the other hand, negative TPI values represent locations that are lower than their surroundings (valleys). TPI values near zero are either flat areas (where the slope is near zero) or areas of constant slope (where the slope of the point is significantly greater than zero).

TPI (Equation 1) compares the elevation of each cell in a DEM to the mean elevation of a specified neighborhood around that cell. Mean elevation is subtracted from the elevation value at the center (Weiss 2001):

$$TPI_i = Z_0 - {\sum_{n-1} Z_n}/{n} \quad (1)$$

where:

Z_0= elevation of the model point under evaluation
Z_n= elevation of grid
n= the total number of surrounding points employed in the evaluation.

Combining TPI at small and large scales allows a variety of nested landforms to be distinguished (Table 2 and Figure 3). The exact breakpoints among classes can be manually chosen to optimize the classification for a particular landscape. As in slope position classifications, additional topographic metrics, such as variances of elevation, slope or aspect within the neighborhoods, may help delineate landforms more accurately (Weiss 2001).

Table 2: Landform classification based on TPI .
(Source: Weiss 2001)

Classes	Description
Canyons, deeply incised streams	Small Neighborhood:$z_o \leq$ -1 Large Neighborhood:$z_o \leq$ -1
Midslope drainages, shallow valleys	Small Neighborhood:$z_o \leq$ -1 Large Neighborhood: -1 <z_o< 1
upland drainages, headwaters	Small Neighborhood:$z_o \leq$ -1 Large Neighborhood:$z_o \geq$ 1
U-shaped valleys	Small Neighborhood: -1 <z_o< 1 Large Neighborhood:$z_o \leq$ -1
Plains small	Neighborhood: -1 <z_o< 1 Large Neighborhood: -1 <z_o< 1

	Slope ≤ 5°
Open slopes	Small Neighborhood: -1 <z_o< 1
	Large Neighborhood: -1 <z_o< 1
	Slope > 5°
Upper slopes, mesas	Small Neighborhood: -1 <z_o< 1
	Large Neighborhood:z_o≥ 1
Local ridges/hills in valleys	Small Neighborhood:z_o≥ 1
	Large Neighborhood:z_o≤ -1
Midslope ridges, small hills in plains	Small Neighborhood:z_o≥ 1
	Large Neighborhood: -1 <z_o< 1
Mountain tops, high ridges	Small Neighborhood:z_o≥ 1
	Large Neighborhood:z_o≥ 1

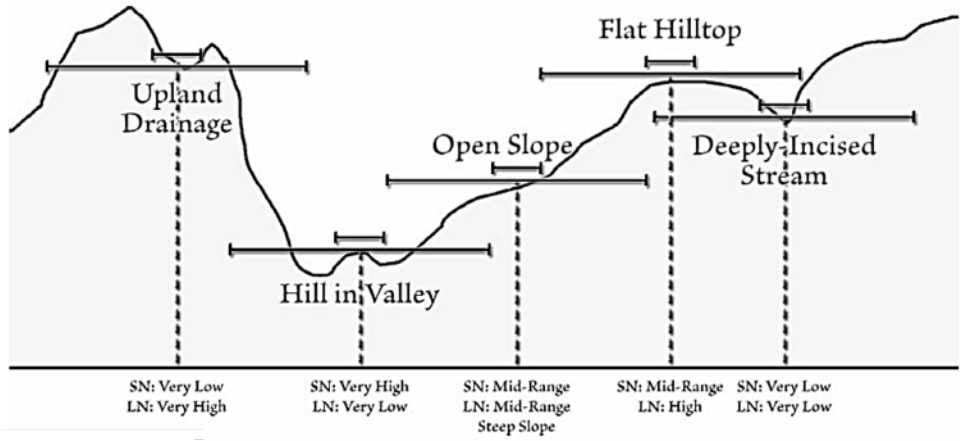

SN: Small neighborhood
LN: large neighborhood

Figure 3: Position of each class on topographic lines (Jenness, 2006).

The classes of canyons, deeply incised streams, midslope and upland drainages, and shallow valleys tend to have strongly negative plane form curvature values. On the other hand, local ridges / hills in valleys, midslope ridges, small hills in plains and mountain tops, and high ridges have strongly positive plane form curvature values.

2.3 Self-Organizing Map (SOM)

SOMs are unsupervised ANNs formed from neurons located on a regular, two-dimensional regular planar array grid (Figure 4). In fact, SOM is based on unsupervised learning, which means that no human intervention is needed during the learning stage and little needs to be known about the characteristics of the input data. SOM offers a solution to apply a number of visualizations linked together (Buza *et al*., 1991). When several visualizations are linked together, scanning through them is very efficient because they are interpreted in a similar way (Dhubkarya et al. 2010). The U-matrix produced from SOM visualizes distances between neighboring map units and thus shows the cluster structure of the map. Samples within the same cluster will be the most similar according to the variables considered (Dhubkarya *et al*., 2010).

The SOM algorithm consists of two individual stages: the competitive and cooperative stages. In the competitive stage, the best matching neuron is selected, while in the cooperative stage, the weights of

the winner are adapted as well as those of its immediate lattice neighbors (Kohonen, 1995). Further explanation for each of the steps is as follows:

1. Competitive stage:

Let A be a lattice of N neurons with weight vectors $w_i = [w_{ij}] \in R_d, W = (w_1, \ldots . w_N)$. All the neurons receive the same input vector$v = [U_1 \ldots U_d] \in V \subset R_d$. For each input v, we select the neuron with the smallest Euclidean distance (''winner-takes-all'', WTA) (Hulle 2012):

$$i^* = arg\ mini \parallel w_i - v \parallel \quad (2)$$

where w_i is neuron weights and v is input vector.

2. Cooperative stage:

The weight update rule in incremental mode is as follows (Hulle 2012):

$$\Delta w_i = \eta \Lambda(I, i*, \sigma\Lambda(t))(v - wi), \forall i \in A \quad (3)$$

where Λ is the neighborhood function, which is a scalar-valued function of the lattice coordinates of neurons i and i^*, r_i and r_i*, mostly a Gaussian:

$$\Lambda(i, i^*) = exp(-\parallel r_i - r_i* \parallel 2 / 2\sigma\Lambda 2) \quad (4)$$

with range $\sigma\Lambda$ (i.e., the standard deviation). The positions r_i are usually taken to be the nodes of a discrete lattice with a regular topology (Hulle 2012).

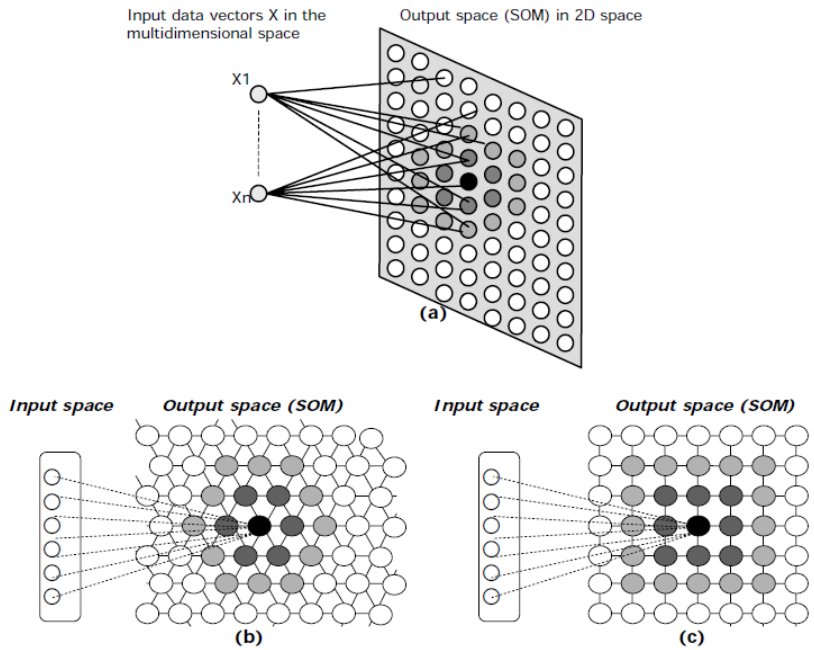

Figure 4: The structure of a SOM network: (a) Selection of a node and adaptation of neighboring nodes to the input data. The SOM grid can be (b) hexagonal or (c) rectangular. The black object indicates the node that was selected as the best match for the input pattern (Dykes 2005).

3. RESULTS & DISCUSSION

3.1 Landform Classification

The TPI maps generated using small and large neighborhoods are shown in Figures 5. TPI is between -94 to 77 and -203 to 260 for 5 and 15 cells respectively (Figure 5). The landform maps generated based on the TPI values are shown in Figure 6.

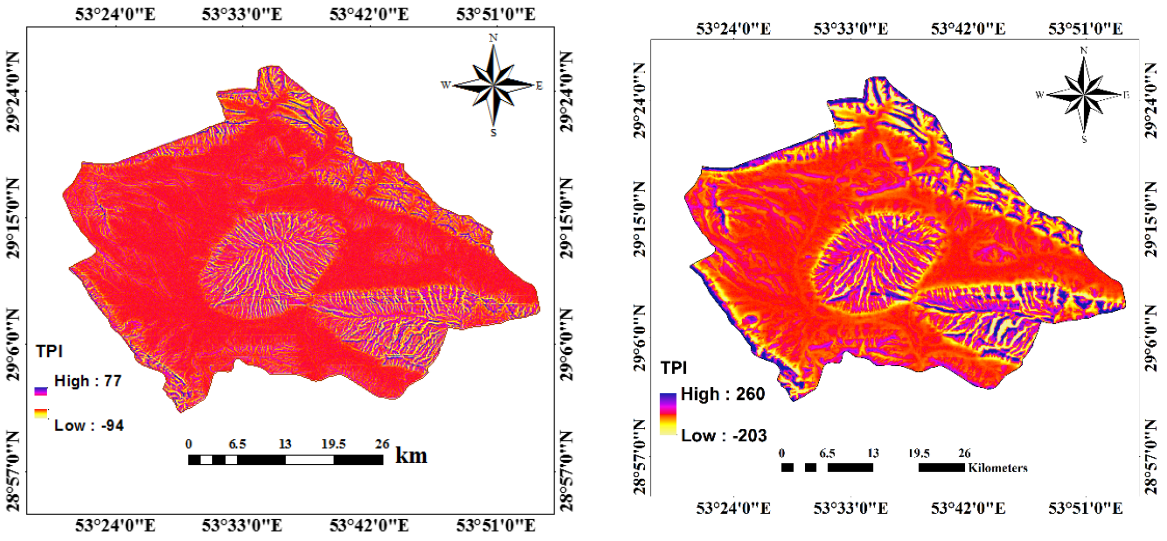

(a) **(b)**

Figure 5: TPI maps generated using (a) small (5 cell) and (b) large (15 cell) neighborhood.

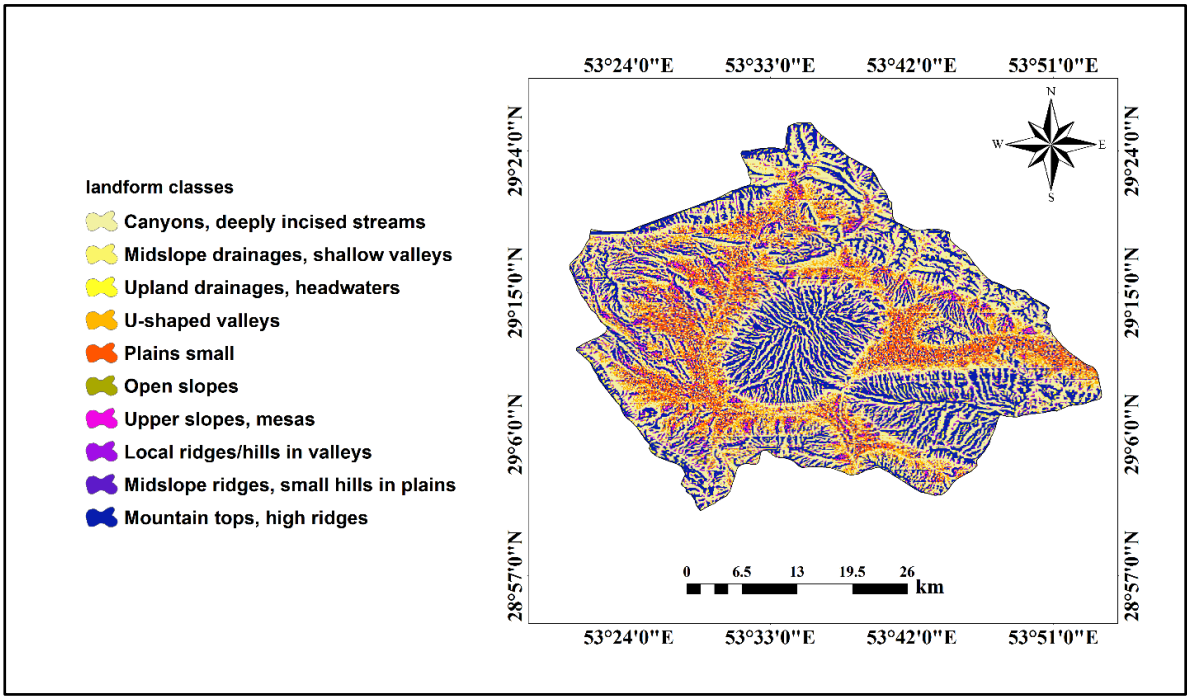

Figure 6: Landform classification using the TPI method.

3.2 SOM for Landform Classification

SOM was applied for the study area to describe the landform classification. The visualizations in Figures 7 and 8 (for landform classification) consist of 16 hexagonal grids, with the U-matrix in the upper left, along with the six component layers (one layer for each morphometric parameter examined in this study). As previously mentioned, the clustering of landform classification used the morphometric parameters of slope, profile, plan, elevation, curvature and aspect (Figure 2).

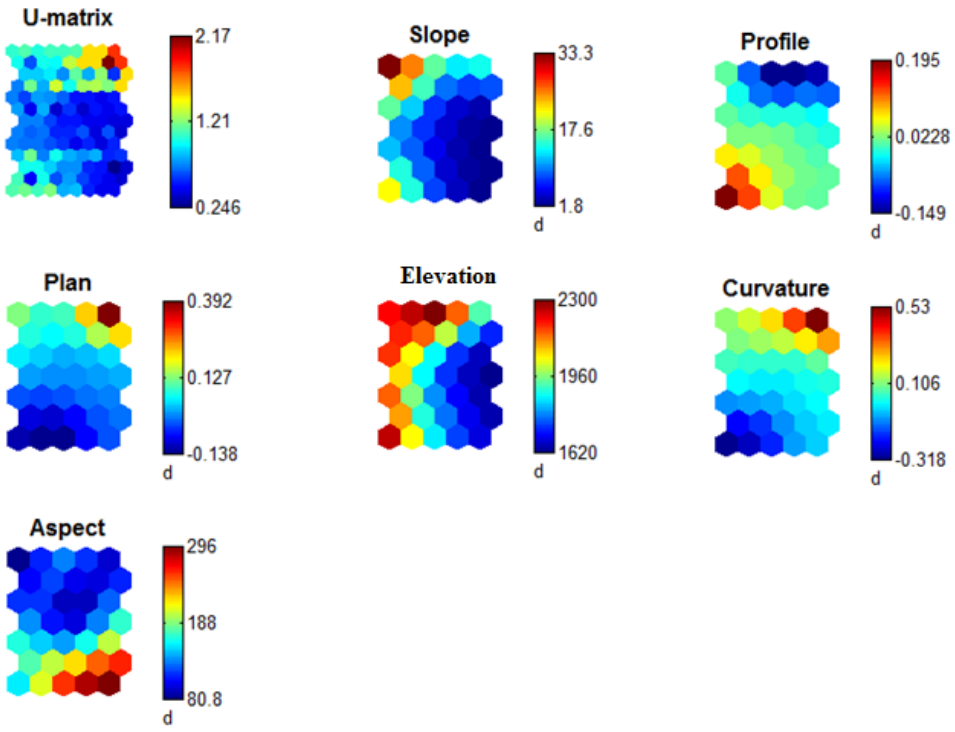

Figure 7: SOM visualization through U-matrix (top left) and the six component layers for landform classification.

According to Figure 7, the six figures are linked by position: in each figure, the hexagon in a certain position corresponds to the same map unit. The legend for each of the hexagons shows the degree of color compared to each other. In the SOM method, similar colors show the direct relationship between the parameters. It can be seen that the elevation and slope are closely related to each other. In addition, profile and curvature are inversely related to each other. The other parameters are not related together.

On the other hand, in the U-matrix, it is easy to see that the bottom rows of the SOM form an almost clear cluster (class A), as shown in the labels in Figure 8(c). The other classes that consist of C, D, E and H form the other clusters (Figure 8c).

As was shown in Figure 8, the numbers written in the hexagons are data that are absorbed by each of the nodes in the neural network (Venna & Kaski, 2001). According to Figure 8, the maximum number of hexagons is 5, indicating that the maximum data in these places is 5. In addition, the minimum number of hexagons is 0, indicating that in these places, there is no data. Based on Figure 8, the principal component (PC) projection showed that the studied data had high density with good distribution. Finally, using the label map (Figure 8c), the study data was classified into five classes for landforms.

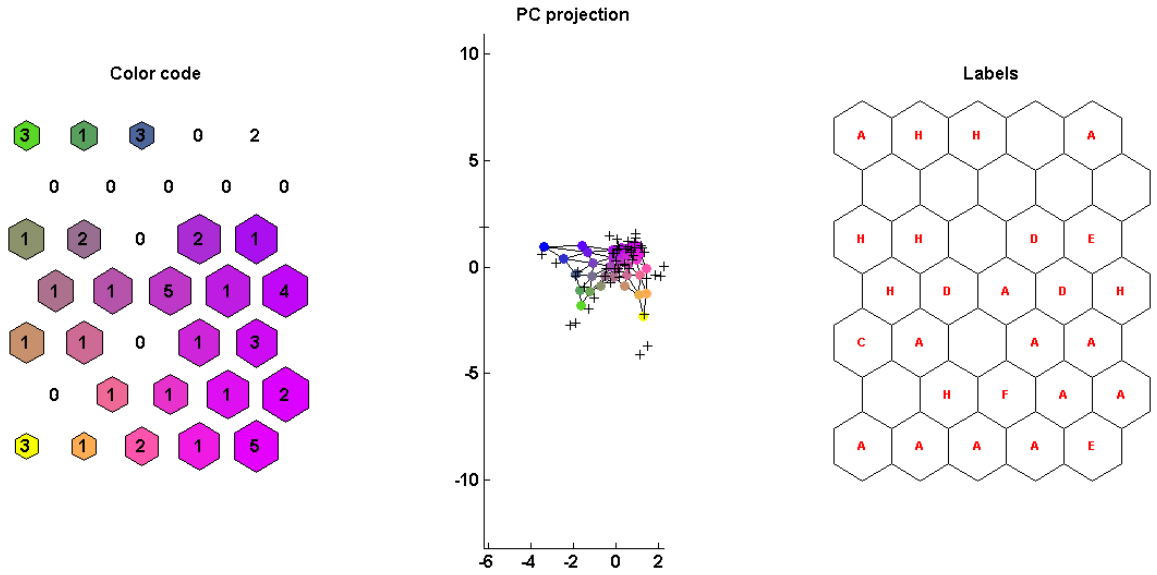

Figure 8. Different visualizations of the clusters obtained from the classification of the morphological variation through SOM: (a) Color code. (b) Principal component projection. (c) Label map with the names of the landform classification.

The characteristics of each group determined by the label map are provided in Table 3. It seems that the five clusters correspond to different terrain forms. From the component planes, the features differentiating the clusters can be seen. In this table, the categorized map units and the corresponding morphometric features are summarized. Cluster 5 corresponds to high slope and elevation, but with different concavity and convexity that consist of ridge landforms. Cluster 3 corresponds to flat areas, possibly plantation areas, with medium elevation and almost flat terrain. Clusters 1, 2 and 4 correspond to channels with different slope conditions.

Table 3: Characteristics of the clusters from the SOM for the landform classification.

Group	Parameters	Slope (°)	Profile (1/m)	Plan (1/m)	Elevation (m)	Curvature (1/m)	Aspect
Cluster 1(A)	Min	Low (<5)	-	-	Medium (1500-2500)	-	North
	Max	High (>23)	+	+	Medium (1500-2500)	+	North
Cluster 4 (C)	Min	Medium (5-16)	-	-	Medium (1500-2500)	-	North
	Max	Medium to high (16-23)	+	+	High (>2500)	+	North
Cluster 2 (D)	Min	Low (<5)	-	-	Medium (1500-2500)	-	East
	Max	Medium (5-16)	+	+	Medium (1500-2500)	+	North
Cluster 3 (E)	Min	Low (<5)	-	-	Low (<1500)	-	East
	Max	Low (<5)	+	+	Medium (1500-2500)	+	Northwest
Cluster 5 (H)	Min	Low (<5)	-	-	Medium (1500-2500)	-	Northeast
	Max	High (>23)	+	+	High (>2500)	+	Northwest

4. CONCLUSION

The purpose of the study was to determine the effectiveness of SOM as a clustering tool for landform classification. In SOM, according to qualitative data, the clustering tendencies of the landforms were investigated using six morphometric parameters (slope, curvature, aspect, elevation, plan and profile). The U- matrix showed that some of the data are closely related to each other, such as elevation and slope. In addition, considering that PC projection represents the data relationship between each other, it was used to determine if the studied data have high density. The results showed that the data have high density and correlation with each other. Finally, using the labels in the SOM method, five classes for the landforms were detected. Cluster 5 corresponds to high slope and elevation but with different concavity and convexity that consist of ridge landforms, while Cluster 3 corresponds to flat areas, possibly planation areas, with medium elevation and almost flat terrain. Clusters 1, 2 and 4 correspond to channels with different slope conditions. Based on the clusters, we can predict that there are five types of main wildlife in the study area.

REFERENCES

Adediran, A.O., Parcharidis, I., Poscolieri, M. & Pavlopoulos, K. (2004) Computer-assisted discrimination of morphological units on north-central Crete (Greece) by applying multivariate statistics to local relief gradients. *Geomorphology*, **58**: 357–370.

Burrough, P.A., van Gaans P.F.M. & MacMillan, R.A. (2000). High resolution landform classification using fuzzy-k means. *Fuzzy Sets and Syst.*, **113**: 37-52.

Buza, A., Mcdonald, J.A., Michalak, J. & Stuetzle, W. (1991). Interactive data visualization using focusing and linking. *Proc. IEEE Conf. Visualization*, pp. 156-63.

Crevenna, A.B., Rodrı´guez, V.T., Sorani, V., Frame, D. & Ortiz, M.A. (2005). Geomorphometric analysis for characterizing landforms in Morelos State, Mexico. *Geomorphology*, **67**: 407–422.

Dehn, M., Grtner, H. & Dikau, R. (2001). Principles of semantic modeling of landform structures. *Comput. Geosci.*, **27**: 1005-1010.

Dhubkarya, D.C., Nagariya, D. & Kapoor, R. (2010). Implementation of a radial basis function Using VHDL. Global J. Comput. Sci. Tech., **10**: 16-19.

Dikau, R. (1989). The application of a digital relief model to landform analysis in geomorphology. *In* Raper, J. (Ed.), *Three-dimensional Applications in Geographical Information Systems*. Taylor & Francis, London, pp. 51–77.

Dikau, R., Brabb, E.E., Mark, R.K. & Pike, R.J. (1995). Morphometric landform analysis of New Mexico. *Zeitschrift für Geomorphologie, N.F.*, **101**: 109-126.

Dykes, J. (2005). *Exploring Geovisualization*. Elsevier, Philadelphia, Pennsylvania.

Ehsani, A.H. & Quiel, F. (2008). Application of self organizing map and SRTM data to characterize yardangs in the Lut desert, Iran. *Remote Sens. Environ.*, **112**: 3284–3294.

Etzelmüller, B. & Sulebak, J.R. (2000). Developments in the use of digital elevation models in periglacial geomorphology and glaciology. Physische Geographie, 41.

Evans I.S. (1979). *An Integrated System of Terrain Analysis and Slope Mapping*. Final report on grant DA-ERO-591-73-60040, University of Durham, Durham.

Ferentinou, M., Hasiotis, T. & Sakellariou, M. (2010). Clustering of geotechnical properties ofmarine sediments through self – organizing maps: An example from the Zakynthos Canyon–Valley system, Greece. *In* Mosher, D., Shipp, C., Chaytor J., Baxter, C., Lee, H. & Urgeles, R. (Ed.), *Advances in Natural and Technological Hazards Research*. Springer, Berlin, pp. 43-54.

Giles, P.T. (1998) Geomorphological signatures: classification of aggregated slope unit objects from digital elevation and remote sensing data. *Earth Surf. Proc. Landforms*, **23**: 581-594.

Ho, T., Yamaguchi, Y. & Umitsu, M. (2013). Rule-based landform classification by combining multi-spectral/temporal satellite data and the SRTM DEM. *Int. J. Geoinform.*, **8**: 27–38.

Hosokawat, M. & Hoshit, T. (2001). Landform classification method using self-organizing map and its application to earthquake damage evaluation. IEEE Geosci. Remote Sens. Symp. 2001 (IGARSS 2001), pp. 1684 – 1686.

Hulle, M.M.V. (2012) Self-organizing maps. Rozenberg, G. (Ed.), *Handbook of Natural Computing*. Springer, Berlin.

Jenness, J. (2006). *Topographic Position Index (tpi_jen.avx) Extension for ArcView 3.x, v. 1.3a*. http://www.jennessent.com/arcview/tpi.htm (Last access date: 20 February 2016).

Kohonen, T. (1995). *Self-Organizing Maps*. Springer, Berlin.

Kohonen, T. (2001). *Self-Organizing Maps, 3rd Ed*. Springer, Berlin.

Lambeck, K. (1996). Sea-level change and shore-line evolution in Aegean Greece since Upper Palaeolithic time. *Antiquity*, **70**: 588-611.

Macmillan, R., Pettapiece, W., Nolan, S. & Goddard, T. (2000). A generic procedure automatically segmenting landforms into landform elements using DEMs, heuristic rules and fuzzy logic. *Fuzzy Sets Syst.*, **113**: 81-109.

Meybeck, M., Green, P. & Vorosmarty, C.J. (2001). A new typology for mountains and other relief classes: an application to global continental water resources and population distribution. *Mount. Res. Dev.*, **21**: 34-45.

Mokarram, M., Seif, A. & Sathyamoorthy, D. (2014). Use of morphometric analysis and self-organizing maps for alluvial fan classification: case study on Ostorankooh altitudes, Iran. *7th IGRSM International Conference on Remote Sensing & GIS (IGRSM 2014)*, 21-22 April 2014, Berjaya Times Square Hotel, Kuala Lumpur.

Moore, I.D. & Nieber, J.L. (1989). Landscape assessment of soil erosion and non-point source pollution. J. Minnesota Acad. Sci., **55**: 18-24.

Moore, I.D., Gessler, P.E., Nielsen, G.A. & Peterson, G.A. (1993a). Soil attribute prediction using terrain analysis. Soil Sci. Soc. Am., **57**: 443-452.

Moore, I.D., Turner, A.K., Wilson, J.P., Jenson, S.K. & Band, L.E. (1993b). GIS and land–surface–subsurface process modeling. *In* Goodchild, M.F., Parks, B.O. & Steyaert, L.T. (Eds.), *Environmental Modeling with GIS*. Oxford University Press, New York, pp. 196-230.

Pike, R.J. (2002). *A Bibliography of Terrain Modeling (Geomorphometry): The Quantitative Representation of Topography-Supplement 4.0*. Open-File Report 02-465, U.S. Geological Survey (USGS), Virginia.

Pike, R.J. & Dikau, R. (1995) Advances in geomorphometry. *Zeitschrift für Geomorphologie*, **101**: 238.

Saadat, H., Bonnell, R., Sharifi, F., Mehuys, G., Namdar, M. & Ale-Ebrahim, S. (2008). Landform classification from a digital elevation model and satellite imagery. Geomorphology, **100**: 453–464.

Samodra, G., Chen, G., Sartohadi, J. & Hadmoko, D.S. (2014). Automated landform classification in a rockfall-prone area, Gunung Kelir, *Java. Earth Surf. Dynam.*, **2**: 339–348.

Schmidt, J. & Hewitt, A. (2004) Fuzzy land element classification from DTMs based on geometry and terrain position. *Geoderma*, **121**: 243–256.

Sulebak, J.R., Etzelmqller, B. & Sollid, J.L. (1997). Landscape regionalization by automatic classification of landform elements. *Norsk Geografisk Tidsskrift*, **51**: 35– 45.

Venna, J. & Kaski, S. (2001). Neighborhood preservation in nonlinear projection methods: An experimental study. *Lect. Notes Comput. Sci.*, **2130**: 485-491.

Weiss, A. (2001). Topographic positions and landforms analysis. *ESRI International User Conference*, San Diego, California, pp. 9-13.

WEAPONS OF MASS DESTRUCTION: A REVIEW OF ITS USE IN HISTORY TO PERPETRATE CHEMICAL OFFENSES

Alba Iannotti[1], Igino Schraffl[2], Carlo Bellecci[1,3], Andrea Malizia[3]*, Orlando Cenciarelli[1,3], Daniele Di Giovanni[1,3], L. Palombi[4] & Pasquale Gaudio[1,3]

[1]International Master Courses in Protection Against CBRNe Events, Department of Industrial Engineering - School of Medicine and Surgery, University of Rome Tor Vergata, Italy
[2]Department of Law, LUMSA University, Rome, Italy
[3]Department of Industrial Engineering, University of Rome Tor Vergata, Italy
[4]Department of Biomedicine and Prevention, School of Medicine and Surgery, Rome, Italy

*Email: malizia@ing.uniroma2.it

ABSTRACT

The use of weapons of mass destruction for military purposes is a problem that has its origins in the early history of humanity. Many substances were used as weapon but the chemical ones were the first to be used in history. The first use of chemical agents dates back to 7th century B.C. during the siege of Cirrha, a Greek city. In the literature of that time there are many examples of the use of chemicals, for example in Thucydides' papers, in which the Greek author describes how the Spartans had burned trees previously soaked with sulphur to produce toxic gases that would have reduced the Plataea city's protections. Unfortunately, their plan failed when the wind direction suddenly changed, poisoning their troops instead. Even the Middle Ages offer many testimonies of the use of chemicals as weapons. A real large-scale use of these substances took place in many other events, for example: during the American Civil war (1861-1865) when General Gilmore used explosive shells against the Confederates. In 1865, when Napoleon used hydrogen for military purposes and in 1900, during the Crimean war, when sulphuric gas was used against the Russian troops near Sevastopol. However, the highest levels of use of chemical agents were achieved during World Wars I and II (WWI and WWII). During these years of wars, the international community deemed necessary to regulate the use of this kind of substances and for this aim a couple of conferences were organized in 1899 and 1907 in The Hague to discuss the regulation of chemical agents' use during war. The most important conference took place in Geneva in 1925 where the Chemical Weapons Convention was born. This work is a review of the historical events involving dangerous chemical agents.

Keywords: *Chemical warfare agents (CWA); World Wars I and II (WWI and WWII); Chemical Weapons Convention (CWC), Organization for the Prohibition of Chemical Weapons (OPCW); toxic*.

1. INTRODUCTION

The term weapons of mass destruction (WMD) was used for the first time on December 28, 1937, in a London Times article on the aerial bombing of Spanish cities by Germany, which noted "*Who can think without horror of what another widespread war would mean, waged as it would be with all the new weapons of mass destruction?*" The United Nations (UN) has been using this term since 1947, defining it as "*atomic explosive weapons, radioactive material weapons, lethal chemical and biological weapons, and any weapons developed in the future which have characteristics comparable in destructive effect to those of the atomic bomb or other weapons mentioned above*" (WHO, 2004). The US administration defined WMD as nuclear, chemical and biological (NBC) weapons, which is the most common use of this concept.

The problems of weapons of mass destruction (WMD): chemical, biological, radiological and nuclear, (CBRN), their proliferation, detection and interdiction, use and deterrence, dismantlement and destruction – are back with a vengeance on the international agenda. The WMD agenda has three interlinked components: non-proliferation, arms control and disarmament. Proliferation refers to the dispersal of weapons, capabilities and technologies. Weapons can be sought for many different reasons, for example, deterrence of enemy attack, defense against attack, compellence of the enemy to one's preferred course of action, leveraging adversary and great power behavior, status and emulation (Thakur, 1999). Specific causes of proliferation are many, diverse and usually rooted in a local security complex. On the supply side, a major proliferation challenge is the globalisation of the arms industry, the flooding of the global arms market and a resulting loosening of supplier constraints.

In history, the worst consequences of war have been the destruction of cities and the great number of victims. These consequences have influenced many legal rules developed to face such particular events. Legal rules that regulate warfare (*ius in bello)* known in present times under the name of international humanitarian law, should conciliate two contrary notions: military need (*ratio belli - necessitas belli*) and demands of humanity (Raicevic, 2001). For these reasons, over the years, some limitations in warfare have been adopted, limitations that concern both people and means of warfare. The most important limitations regard the use of weapons, it is prohibited especially to use weapons that could cause non-combatants' death, civil targets' destruction or unnecessary increase of suffering of combatants and disproportional destruction of military targets. Chemical weapons (CW) are one of the means of warfare and the prohibition of those weapons has been present since ancient times in international law. CW could be, in the shortest possible way, defined as "*each weapon containing chemical substances, nonliving matters capable of causing consequences against people, animals and plants and infrastructures*" (Raicevic, 2001).

The use of chemicals as a means of war is almost as old as human history (poisoned arrows, arsenic smoke and noxious fumes, for example). As with other types of weaponry, the means, range, accuracy and lethality of CW and their delivery systems increased exponentially over the course of the last century. The efficient harnessing of CW for large-scale deployment and use owes much to modern industrial processes and organization (Thakur & Ere, 2006). A CW attack on a city could be expected to produce thousands of deaths. During World War I, successful gas attacks would use tons of gas and produce hundreds of thousands of deaths and thousands of injured. An Office of Technology Assessment report suggests 1,000 kg of sarin gas aerially dispersed on a city with a density of 3,000 to 10,000 people per square kilometer would result in 300 to 8,000 deaths, depending on the climatic conditions at the time of attack (OTA, 1993).

The use of non-conventional agents (like chemicals) to perpetrate an unconventional event is not only a past but also a recent reality. The solutions to such problems are various, and the Quantum Electronics and Plasma Physics Research Group (University of Rome Tor Vergata) has been conducting research to develop innovative hardware solutions (Bellecci *et al*., 2009; Gaudio *et al*., 2010; Pazienza *et al*., 2013, 2014; Malizia, Camplani *et al*., 2014; Carestia, Pizzoferrato, Cenciarelli *et al*., 2014; Sassolini *et al*., 2014; Gelfusa *et al*., 2015). The group is also working on a new Decision Support System (DSS) (Gelfusa *et al*., 2014; Malizia, Carestia *et al*., 2014; Gaudio *et al*., 2014; Lupelli *et al*., 2014; Carestia, Pizzoferrato, Gelfusa *et al*., 2014; Carestia *et al*., 2015; Ciparisse *et al*., 2015), and analyzing particular events using state of the art techniques and technologies in order to understand and address the problems (Malizia *et al*., 2010; Gaudio *et al*., 2011; Cacciotti *et al*., 2014; Cenciarelli *et al*., 2014; Cenciarelli, Gabbarini *et al*., 2015; Cenciarelli, Pietropaoli *et al*., 2015; Baldassi *et al*., 2016).

The success of a CW attack depends on the purity of the agent; climatic factors, such as wind, cloud cover, temperature, and precipitation; the physical properties of the chemical, including density, vapor pressure, and boiling point; persistence in the environment; and delivery mechanism (Caldicott, 2002). Moreover, the lethality of a CW attack depends on whether and how the targets are defended.

2. CHEMICAL WEAPONS BEFORE WORLD WAR I (WWI)

The use of certain chemical agents in warfare has been known for a long time. Chemical agents emerged considerably prior to biological and nuclear weapons. However, the forms of chemical agents and the modes of their use were primitive. In spite of the fact that a great number of wars had been waged, it was only in some of them that the use of chemical agents was recorded. It is well known that the Chinese in olden days used smoke preparations – "*pungent substances that cause nausea and disgust*". Poisons have often been used for criminal poisoning of people. In the struggle of power and heritage, people were fighting among each other by using various poisonous agents, and poisons were also used for war purposes. For example, arsenic smoke clouds were used to defend Belgrade against the Turks in 1456 (SIPRI, 1971). There were also examples of the use of chemical agents in war in the modern times such as the American civil war and during the Boer War in 1900 when explosive shells filled with a poisonous gas were employed. These mentioned cases of use of chemical agents cannot be considered a usual form of warfare, but accidental and periodical events. Chemical agents used during wars were not intended for military needs, it was their incidental purpose. There were no special devices for their use. Therefore, CW, in the ordinary meaning of the word, cannot be spoken of during this period.

The history of humankind does not recognize such an odious form of warfare as is the use of poisonous substances for military purposes. The use of such agents was condemned for numerous reasons. They were considered perfidious combat agents inconsistent with military chivalry and, accordingly, should not be used by combatants. Their use had been condemned long before, for instance by ancient writers, such as Philius, Ulpian, Tacitus and Claudianus. The Roman Senate stuck to the principle that war should be waged using weapons but not poisons, also Hugo Grotius thought that it was "forbidden to kill anybody by means of poison" and that "it is not allowed to poison weapons and water". Initially, prohibitions were being established under the customary law to gradually take, later on, the form of a treaty (Schindler & Toman, 1973).

The first written treaty under which the use of chemical agents in warfare was limited is a Franco-German agreement of 1675 concluded in Strasbourg. The use of poisoned shells was prohibited in warfare under this agreement on bilateral grounds. The prohibition of the use of chemical substances in warfare is also contained in Lieber's instructions of 1863 also known as Lieber Code, an instruction signed by President Abraham Lincoln to the Union Forces of the United States during the American Civil War that dictated how soldiers should conduct themselves in wartime. Francis Lieber, an international law scholar-professor, prepared it. "Lieber's Instructions" represent the first attempt to codify the laws of war (Schindler & Toman, 1973). That prohibition is discussed twice in these Instructions. Part I includes a general prohibition of the use of poisons in war (Article 16). In Part III of the Instructions (Article 70), that prohibition is partially made precise, and this Article reads: "The use of poisons in any manner, be it to poison wells, or food or arms, is wholly excluded from modern warfare. He that uses it puts himself out of the pale of the law and usages of war." The first deed at a multilateral level that contains a prohibition of the use of poisonous substances in war is the Brussels Declaration of 1874 (Schindler & Toman, 1973). It was not an agreement in the ordinary meaning of the term, it remained at the stage of a project, but its provisions were important for the future development of the law of war. Article 12 of the Declaration provides that belligerent powers shall not have full liberty in choosing means and methods of fight against the enemy. Article 13 prohibits certain means and methods of warfare among which is the prohibition of the use of "poison and poisoned weapons". The ban of the use of poison in war was the conclusion that the Declaration would reach.

The two Hague Conventions are the other documents under which the use of chemical agents in warfare is prohibited. The relevant provisions are contained in the annexes to these Conventions, which represent their most important parts and are known under the name Hague Regulations. The provisions concerning the prohibition of poisonous substances are identical in both Regulations (1899 and 1907). The prohibition of the use of poisonous substances in warfare is regulated under Article 23 of these Regulations. Two paragraphs of this Article are essential for that prohibition, paragraphs a

and e. There is a general prohibition to employ arms, projectiles or material of such a nature as to cause unnecessary injury (paragraph e): since poisonous substances, in view of their effects, can be considered means that cause unnecessary injury, they fall under this paragraph as well. Paragraph a of the same Article explicitly stipulates that the utilization of "poisons and poisoned weapons" is prohibited. In addition, a Declaration concerning Asphyxiating Gases was discussed and the prohibition is formulated as follows: "The contracting powers prohibit the use of projectiles the sole objects of which is the diffusion of asphyxiating or deleterious gases". The particularity of these statements was the prohibition of weapons not yet in existence at that time, but the creation of which could be envisaged in the future to come. At the time when the Declaration was adopted, projectiles filled with deleterious gases were still an idea. These were the legal norms in the field of prohibitions of the use of CW at the outbreak of WWI, when the relevant norms gained a practical value (Thakur & Ere, 2006).

3. FROM WWI TO THE NEW MILLENNIUM

3.1 WWI

WWI has been the turning point in the use of chemical agents as weapons. A large quantity of chemical agents were used resulting in many victims. Chemical agents were used by the Germans and the allies as well. The turning point occurred in Ypres on April 22, 1915 when Germany used bottles filled with chlorine against the Allied forces. As a consequence of that attack there were 15,000 wounded soldiers on the side of Allied forces, out of which 5,000 were killed. This new and unexpected attack provoked great losses because the soldiers were not well equipped for this substance. The Allied forces, as a response to the German attack, began using CW too. At this point the war made a big progress, CW were used more and more often. New devices for the chemical and poisonous gases dispersion were created and improved in this period. More than 50 different toxic compounds amounting to 125,000 tons are supposed to have been used by Germany and the Triple Entente over the period from 1914 to 1918. Such frequent use of poisonous gases resulted in mass victims (SIPRI, 1971). Table 1 shows the number of said victims.

Table 1: Number of victims of Chemical agents during WWI. (Modified from SIPRI, 1971)

State	Total casualties from Chemical agents (fatal and nonfatal)	Fatal causalities from Chemical agents
Germany	200,000	9,000
France	190,000	8,000
Great Britain	189,000	8,100
Austria-Hungary	100,000	3,000
Italy	60,000	4,600
Russia	475,000	56,000
USA	73,000	1,500
Belgium and Portugal	10,000	1,000
Total	1,297,000	91,200

3.2 From WWI to World War II (WWII)

After WWI, as a consequence of the use of new methods of war, the field of international law radically changed to try to regulate the use of CW in warfare. One group of authors condemned the use of CW and considered it a violation of international law, while another group held that the use of those weapons did not constitute a violation of the existing legal prohibitions. The German law theory was particularly persistent in justifying the use of CW, and this may be because they were one of the

first to use CW. Some argued that Germany respected the rules of the Hague Declaration Concerning Asphyxiating Gases until 1916, because the German army used bottles to spread poisonous gases that could not be classified as "projectiles", which were prohibited under the Declaration. It was also pointed out that the projectiles used were filled with explosive in addition to a chemical charge, for which reason they were not covered by the Hague Declaration, because the spreading of asphyxiating gases was not their "only" purpose. The starting point is that the sources of the law of war are not made up only by treaty rules, but customary law as well.

During WWI, the limitations about the use of chemicals and poisonous gases were general and this is why the need to conclude a treaty was felt after the War whose only purpose should be to regulate the prohibition of the use of CW. This was done in 1925 with the adoption of the Geneva Protocol for the Prohibition of the Use in War of Asphyxiating, Poisonous or other Gases and of Bacteriological Methods of Warfare. This Protocol was preceded by two international deeds containing provisions limiting the use of CW. The first of them is the Versailles Peace Treaty, the second act is the Washington Conference, also known as Treaty on the Use of Submarines and Noxious Gases in Warfare between France, Italy, Japan, United Kingdom and United States (Washington D.C. February 6, 1922). The Treaty did not enter into force, because France did not ratify it. Article 5 reads: "*The use in war of asphyxiating, poisonous and other similar gases having been declared in treaties to which a majority of the civilized Powers are parties. The Signatory Powers declare their assent to such prohibition, agree to be bound thereby as between themselves and invite all other civilized nations to adhere thereto."* This Article is important in that it confirms that the use of CW had already been prohibited under customary law. As to the 1925 Geneva Protocol itself, its purpose was to eliminate the imperfections and voids existing in the former prohibitions to use CW. Legal regulations should be harmonized under it with the new technological accomplishments related to the use of CW, such as airplanes, airplane bombs, etc. The Protocol contains a general formulation of the prohibition of the use of chemicals without indicating the means of their possible use.

Some would argue that only the use of CW was prohibited, but not their improvement, production and transfer, nor was the destruction of existing CW requested. The risk that CW were used would be greatly reduced if they were to be eliminated, by destroying the existing stocks and prohibiting their further improvement, production and transfer. The unlimited possibility of making observations to the Protocol's provisions may be considered an imperfection; in fact, this possibility was widely used by different states to frequently hinder the purpose and spirit of the Protocol, for instance, using CW against the non-signatory states, or to seek revenge and respond in kind if attacked with CW by another state. The States kept on accumulating large stockpiles justifying them by the necessity of creating capacities of countering the -internationally illegal - use of CW of potential rivals (Raicevin, 2001).

It happened in the Italo - Ethiopian war of 1935-1936 and was a violation of the Geneva Protocol, because both Italy and Ethiopia were among its signatory states. Italy used around 700 tons of chemical agents, mostly delivered by the Italian air force (SIPRI, 1971). During those attacks, in addition to soldiers, there were civilian victims as well. Reports on horrible consequences were obtained mainly from physicians, representatives of national organizations of the Red Cross and journalists. John Melly, head of a field hospital of the British Red Cross, describes that war as follows: "It is not a war, it is not even a slaughter – it is a torture of thousands of defenseless men, women and children" (Baudendistel, 1998). Poisonous gases were not only used during the 1935-1936 war, but also during the subsequent occupation against Ethiopian rebels. The Italians justified the use of CW by necessary reprisals against the brutality committed by Ethiopian troops over Italian soldiers.

The use of CW was recorded also in the Sino-Japanese war of 1937-1945. The Japanese army used different chemical agents several times. Over the period between the two World Wars, further investigations and developments of CW were continued. New poisonous gases were produced which were several times stronger than those used in World War I. The improvement of CW, their mass

production was commenced specially prior to the outbreak of the War in order to lead the war more effectively (Raicevin, 2001).

During WWI, the use of CW in war became systematic and some European army began attacking the enemy with those agents. Ypres, in 1915, was the first battle fought with the use of liquid chlorine. At the end of WWI, some nations tried to stop the crazy stroke to find the perfect chemical/biological agent to give the final rush in future wars, therefore in 1925 a specific convention for chemical and biological weapons was prepared. The discussion began in 1921, when the League of Nations considered banning the use of CW in war. After the experience of WWI, the Geneva Protocol in 1925 was prepared. All the great powers and most of other nations ratified the Geneva Protocol that entered into force on February 8, 1928. The Protocol is considered an agreement that forbids the use of chemical and biological weapons except in case of retaliation.

3.3 WWII

At the beginning of WWII, the states involved had their own programs to create and use chemical and biological weapons. In the period prior to the CW Convention (CWC), large stockpiles of CW were in possession of both belligerent sides at the outbreak of World War II and their production continued during the war. However, there was no mass use of these agents during this war and there are several reasons stated for it. One of the reasons for non-use was some statements made during the war. Great Britain and France obligated themselves under the joint declaration of September 3, 1939 and the government of Nazi Germany under the declaration of September 9, 1939, that they will strictly observe the provisions of the Geneva Protocol, under the condition that the other party would do the same.

In addition, the reasons of military nature contributed to the non-use of CW. These reasons partially explain why the prohibition of the use of CW was the most observed prohibition in World War II (in contrast to the prohibition with reference to civilians, wounded, prisoners and targeted premises), but it is still uncertain why the use of CW were deterred. After World War II, due to the advent of nuclear weapons, the interest of great powers in CW diminished for some time. Greater importance to CW was attached by states that had no nuclear weapons. However, after the nuclear balance had been redressed the interest in CW was again revived.

3.4 From WWII Until the New Millennium

There were accusations that in certain wars waged after 1945 some belligerent states used CW. However, few of those accusations were proved before international entities, and in even fewer cases, the accused party admitted to have used such weapons. Below are some of the wars in which CW were used (OPCW, 1999):

1945-1949: *China*. During the Chinese civil war, both parties to the conflict heavily accused each other of using chemical agents;

1947: *Indochina*. The French forces were accused of using CW in battles against the Vietnamese nationalists. However, such accusations were refuted by French officials;

1948: *Israel*. In January 1949, the Israeli military officials refuted the accusations by Egypt on the supposed use of CW against Egyptian troops;

1949: *Greece*. "Tanjug", the Yugoslav news agency reported that a poisonous gas was used by the governmental entities against the war forces in Peloponnesus. However, the Greek defense minister stated that only excitant gases had been used for the purpose of expelling guerrillas from the caves;

1951-1952: *Korea*. The US were accused of using CW several times in that conflict, the heaviest attack being that on May 6, 1951, when the American bombardiers B-29 dropped bombs filled with poisonous gases nearby the city of Nampo;

1957: *Cuba*. Cuban emigrants requested inspection by the United Nations because of a supposed use of chemical agents –mustard- by the Cuban government against the guerrillas;

1957: *Algeria*. The French forces were accused of using chemical agents against the Algerian rebels. The accusations were refuted by the French commanders in the field;

1958: *China*. Radio Peking accused the Chinese nationalist forces of using shells filled with chemical agents when bombing the Chinese people's army. On that occasion, the Peking defense minister threatened to take revenge in case of continued attacks. The nationalists and American authorities in Taipei refuted those statements;

1963-1967: *Yemen*. There were several reports that the Egyptian forces had used CW during their intervention in the Yemen civil war. All the accusations were refuted by Egypt, considering them to be propaganda against Egypt;

1961-1973: *Indochina*. There were several reports on the use of CW during the war in Vietnam. The mass use of herbicides and excitant gases by American troops and the South- Vietnamese army was proved by sources in the US. However, the US emphasized the fact that the use of excitant gases and herbicides was not prohibited either under customary law or under the Geneva Protocol - the signatory state of which US was not, but observed its provisions. US was supported in such interpretation of law by some states, particularly by Great Britain (SIPRI, 1973).

There were opposing views, however the majority of states supported the US at that time. Within the United Nations, and elsewhere, it was emphasized that the use of any kind of chemical and biological weapons was prohibited in warfare. Such attitude was adopted by the General Assembly of the United Nations under its Resolution 2603 of 1969. Laid down in which is that the use of: "*Any chemical agents for warfare – chemical substances, whether gaseous, liquid or solid – which might be employed because of their direct toxic effects on men, animals or plants*" in armed conflicts is prohibited under the Geneva Protocol of 1925. There were accusations that the US in that war used mortal poisonous gases. However, the US refuted the use of such poisons. The use of herbicides and excitant gases in Vietnam caused serious consequences. The use of poisonous gases was particularly severely criticized by the member states of the Warsaw Pact and the effects of that use were widely reported by the press of those states. The American army is supposed to have dropped 100,000 tons of poisonous matters in Vietnam. Around two million people were afflicted by the consequences of the use of these poisonous matters, not only the Vietnamese, but the Americans too. About one million of Vietnamese died of starvation due to destruction of rice fields and other agricultural products. More than 43 percent of the cultivable soil in Vietnam was unusable due to the effects of herbicides. The use of poisonous gases resulted in a number of inborn defects with the children born after the war, both in Vietnam and with the children of the Americans who participated in the Vietnamese war.

1975: *Laos*. Vietnamese forces, supported by Soviet experts, were suspected to have used chemical agents in Laos;

1978-1980: *Laos, Cambodia and Afghanistan*. The US and the United Nations point to the use of CW in Laos and Cambodia and then in Afghanistan.

1980- 1988: *Iraqi-Iranian war*. Starting from 1984, Iran permanently accused Iraq of the use of CW. Iraq sent a number of victims of those attacks to Western Europe for treatment. A committee for establishing the supposed use of CW by Iraq was set up by the United Nations Secretary General and

that team confirmed the accusations of Iran. In addition, Iran was accused by Iraq by the end of the war to have used CW weapons as well, but the accusations were not confirmed.

1992-1995: *War in Bosnia and Herzegovina* (Stock *et al.*, 1996). During the war there were mutual accusations that each party to the conflict -Serbs, Moslems and Croats- used CW in certain battles. However, the independent experts did not confirm such accusations.

In addition to the use in warfare, CW become attractive for terrorist as well. After the terrorist use of a poisonous gas by a religious sect in the Tokyo under-ground, the international community became aware of the great danger if CW reached the hands of terrorists (Stock *et al.*, 1996).

Considerably contributing to the CW prohibition negotiations were particularly the Iraqi-Iranian war and the Tokyo terrorist attack. After World War II until the adoption of the CWC in 1993, no international agreement was concluded referring to CW. However, it does not mean that no efforts have been made in the domain of controlling that kind of weapons. The greatest efforts have been made within the United Nations and the International Red Cross.

The following resolutions of the General Assembly of the United Nations with respect to CW are listed below: Resolution 2162B (XXI) of 1966; Resolution 2444 and Resolution 2454A (XXIII) of 1968 and Resolution 2603 (XXIV) of 1969. Under these Resolutions the existing prohibition of the use of CW is pointed out by the General Assembly of the United Nations, states are called up to observe this prohibition and those states that have not joined the treaties are called up to do so. Also worth mentioning is a report of a group of experts (United Nations, 1969), set up at the request of the United Nations Secretary General in 1969, on the consequences of possible use of CW, in which it is ascertained that, if they should widely be used in warfare, no one could predict how lasting the consequences would be.

In the Draft Rules for the Limitation of the Dangers Incurred by the Civilian Population in Time of War, drew up by the International Committee of the Red Cross in 1955, the use of asphyxiating, poisonous and similar gases, bacteriological agents as well as similar liquids, substances and methods are prohibited. In addition, appeals from many international conferences of the Red Cross have been made to all states to join the Geneva Protocol of 1925.

An appeal of similar content was also made at the conference on human rights held in 1968 in Teheran. However, a need was being noticed to make an international agreement that would eliminate imperfections of the existing rules in the domain of prohibition of the use of CW. For that reason, negotiations were taken up in 1968 on the convention under which prohibition of CW would be regulated, and they would, as it turned out, last until 1993 when the Convention on the Prohibition of the Development, Production, Stockpiling and Use of CW and on Their Destruction was signed.

4. GENESIS AND HISTORICAL DEVELOPMENT

4.1 From the End of the 19th Century to the First Years of the 20th Century

The history of the serious efforts to achieve chemical disarmament that culminated in the conclusion of the CWC began more than a century ago. Although toxic chemicals have been used as a method of warfare throughout the ages, it is clear from some of the earliest recorded incidents that such weapons have always been viewed as particularly abhorrent. An international peace conference held in The Hague in 1899 led to the signing of an agreement that prohibited the use of projectiles filled with poison gas.

The efforts of the twentieth century were rooted in the 1899 Hague Peace Conference. The contracting parties to the 1899 Hague Conventions declared their agreement to abstain from the 'use of projectiles, the sole object of which is the diffusion of asphyxiating or deleterious gases'. Their

intentions unfortunately proved futile. The rules of warfare agreed at the Hague Conference and its successor (the 1899 and 1907 Hague Regulations) prohibited the use of poisoned weapons. Nonetheless, CW was used on a massive scale during WWI, resulting in more than 100,000 fatalities and a million casualties (Gay, 2001)

The result of this renewed global commitment was the 1925 Geneva Protocol for the Prohibition of the Use of Asphyxiating, Poisonous or Other Gases, and of Bacteriological Methods of Warfare. However, the Geneva Protocol does not prohibit the development, production or possession of CW. It only bans the use of chemical and bacteriological (biological) weapons in war. Furthermore, many countries signed the Protocol with reservations permitting them to use CW against countries that had not joined the Protocol or to respond in kind if attacked with CW. Since the Geneva Protocol has been in force, some of these States Parties have dropped their reservations and accepted an absolute ban on the use of chemical and biological weapons. During the first half of the twentieth century, many developed countries spent considerable resources on the development of CW, particularly after the discovery of powerful nerve gases renewed interest in the field. A number of countries used CW in the inter-war period, and all the major powers involved in World War II anticipated that large-scale chemical warfare would take place. Contrary to expectations, however, CW were never used in Europe in World War II. The reasons are uncertain, and historians still debate whether it was fear of retaliation in kind, the level of protection of enemy troops, or moral reasons that deterred their use. The fate of some of the stockpiles built up in anticipation of World War II is also uncertain. Many CW were abandoned, buried or simply dumped at sea. In any event, following World War II, and with the advent of the nuclear debate, several countries gradually came to the realization that the marginal value of having CW in their arsenals was limited, while the threat posed by the availability and proliferation of such weapons made a comprehensive ban desirable. At that time, the issues of chemical and biological weapons disarmament were linked to each other. Both issues became the subject of active consideration when, in 1968, Sweden was able to include them on the agenda of the multilateral Geneva disarmament conference. At that time, the conference was called the Eighteen Nations Disarmament Committee (ENDC) (Thakur, 1999; Thakur & Ere, 2006).

4.2 From the 1970s to the 21st Century

Shortly thereafter, the negotiations on biological and CW issues diverged. In 1969, the United Kingdom tabled a draft biological weapons disarmament treaty. After several modifications that reduced its effectiveness, the draft Biological Weapons Convention was agreed upon in the disarmament conference, and was endorsed by the United Nations General Assembly. The treaty opened for signature in 1972 and entered into force in 1975. The Biological Weapons Convention was an incremental step forward in the commitment to achieving a CW ban. Each State Party to this Convention affirms the recognized objective of effective prohibition of CW and, to this end, undertakes to continue negotiations in good faith with a view to reaching early agreement on effective measures for the prohibition of their development, production and stockpiling, and destruction. In addition, appropriate measures concerning equipment and means of delivery specifically designed for the production or use of chemical agents for weapons purposes are necessary. The issue of CW was therefore retained on the agenda of the Geneva Conference, and various states tabled drafts during the 1970s. This era also saw the announcement of a joint US–Soviet initiative on CW, which was to be submitted to the Geneva Conference. A US–Soviet working group set up during this period began discussing some key ideas, which eventually formed the building blocks of the CWC. These included the need to control the precursors of CW, to establish mechanisms such as a conference or committee of all states parties and a secretariat to oversee the implementation of the treaty, and to use routine and challenge inspections as part of the verification regime. In 1978, the Geneva conference -it was renamed as the Conference on Disarmament in 1980- was restructured. Its membership increased to 40, and the chairmanship was to rotate among the members. The Conference decided in March of that year to establish an ad hoc working group on CW, which was required to 'define, through substantive examination, issues to be dealt with in the negotiations' on the Convention. Significant developments in the elaboration of the draft Convention were made in 1984. The United States submitted a new

draft text, which proposed intrusive verification measures, including mandatory challenge inspections. The negotiations received a new impetus when the Secretary-General of the United Nations announced that CW had been used by Iraq in its war against Iran. The Conference then agreed to begin elaborating a ban on CW, and mandated the ad hoc working group accordingly. The group worked based on a "rolling text" of the Convention on which areas of consensus and disagreement were reflected. Beginning in 1986, the global chemical industry actively participated in these negotiations. Unlike the BWC, the negotiators of a CW ban reached an understanding that this ban would be subject to international verification. To this end, trial inspections of both industrial and military facilities were undertaken, starting in late 1988. With the thawing of relations between the United States and the Soviet Union, there were a number of major breakthroughs in the negotiations on the Convention. In August 1987, the USSR indicated its willingness to accept, and even extend, the proposals for an intrusive verification regime contained in the 1984 US draft treaty. In the meantime, photographs of a chemical attack on civilians in Northern Iraq in March 1988 were widely published in the media. The international community reacted with repugnance against this use of CW, and within the Conference on Disarmament, the momentum for the conclusion of negotiations increased. In September 1989, President George Bush announced the new US position to the UN General Assembly: instead of total verifiability, the United States would seek "*a level of verification that gives us confidence to go forward.*" In 1990, the United States and the Soviet Union also signed a bilateral agreement on CW, under which the two countries agreed not to produce CW, to reduce their stocks of CW to 20% of current holdings; and to begin destruction in 1992. It was also agreed that neither country would have more than 5000 tons of chemical agents by 2002. This agreement never entered into force; it nevertheless marked a willingness on the part of the two major possessors of CW to work together to eliminate this class of weaponry (Thakur, 1999; Thakur & Ere, 2006).

While the differences between the Americans and Soviets appeared to be diminishing, other issues gained prominence. Several Arab countries, for example, linked chemical disarmament to progress on nuclear disarmament. Developing countries were generally concerned about whether the Convention would carry any benefits for them. Various new provisions were therefore developed for inclusion in the text of the Convention during the final years of the negotiations, such as:

- Assistance to victims of CW use;
- The exemption of some sectors of the chemical industry from routine inspections;
- The imposition of obligations on States Parties in relation to abandoned CW;
- Promise on the part of several developed countries, known collectively as the "Australia Group", to review export controls and other barriers to trade in chemicals.

On the whole, the last "concession" from the industrialized countries, embodied in Article XI on economic and technological development, was probably the key to obtaining broad support for the Convention, since for a number of developing countries, free trade in chemicals for purposes not prohibited under the Convention was the only important issue. The solution that was found is perhaps best captured in the statement of the Australian representative to the plenary session of the Conference on Disarmament on August 6, 1992 (OPCW, 2016).

"*The members of the Australia Group undertook to review, in the light of the implementation of the Convention, the measures that they will take to prevent the spread of chemical substances and equipment for purposes contrary to the objectives of the Convention*" (OPCW, 2016). The aim was removing such measures for the benefit of States Parties to the Convention acting in full compliance with their obligations under the Convention. Paragraph 40 of the Report of the Ad Hoc Committee on CW to the Conference on Disarmament, CD/1170, dated August 26, 1992.

In 1992, another obstacle to agreement on the Convention was removed when the United States renounced its previous insistence on retaining the option of retaliation in kind, and accordingly dropped its demand for the right to retain security stockpiles. There was a strong push to conclude the CWC. This was affirmed when President Bush called for, and obtained agreement on, a one-year

deadline for the completion of negotiations. It was clear to everyone involved that 1992 offered a window of opportunity for agreeing on a text for the treaty. The Chairman of the ad hoc Committee on CW moved quickly and tabled a draft Convention which incorporated the latest 'rolling text' and possible compromise solutions. After two more revisions, the draft convention was approved by most delegations, and was transmitted to the Conference in the summer of 1992. The Conference on Disarmament adopted the draft text on September 3, 1992 and transmitted it in its Report to the UN General Assembly. The text of the Convention was commended by the General Assembly in December 1992, with the request to the UN Secretary-General, as Depositary of the Convention, that it be opened for signature in Paris on January 13, 1993. A total number of 130 States signed the Convention within the first two days and it was subsequently deposited with the United Nations Secretary-General in New York. Recognizing that considerable preparations were required, and that a number of outstanding issues still remained to be resolved before the Convention could enter into force, the signatory states in Paris approved a resolution -the 'Paris Resolution'- to set up a 'Preparatory Commission' for the future Organization for the Prohibition of CW.

Under the General Assembly resolution commending the text of the Convention, the UN Secretary-General was also requested to provide the services required by the signatory states to initiate the work of the Preparatory Commission. Accordingly, the Paris Resolution mandated the UN Secretary-General to convene the Preparatory Commission for its first session within 30 days of the fiftieth signature of the Convention. Since this threshold, number was easily exceeded at the signing ceremony in Paris, the inaugural session of the Preparatory Commission was held shortly thereafter, on February 8, 1993, in The Hague, the Netherlands, and the seat of the future Organization. As mandated in the Paris Resolution, the Preparatory Commission immediately established a Provisional Technical Secretariat to assist its work, and to prepare for the eventual Secretariat of the Organization for the Prohibition of Chemical Weapons (OPCW). The Preparatory Commission stayed in existence from 1993 until shortly after the Convention entered into force on April 29, 1997. According to the terms of the Convention, the CWC would enter into force 180 days after the 65th country ratified the treaty. To prepare for the treaty's entry into force and the implementation of the verification regime, a Preparatory Commission was established in 1993. The work of the Preparatory Commission, as described in the Paris Resolution, was to prepare the 1st Session of the Conference of the States Parties after Entry into Force, to make all necessary practical preparations for the implementation, and to finalize the work and the necessary procedures and guidelines needed for its implementation. These activities can be broadly categorized as developing the operational procedures for the CW's Verification regime and other operations; drafting the program and budget of the OPCW; and establishing the infrastructure and internal functional rules for the OPCW Secretariat. The Preparatory Commission functioned primarily through two working groups, one of which was tasked with considering administrative and organizational matters, while the other was assigned the responsibility for issues relating to verification and technical cooperation and assistance. Other bodies were also created to assist the work of the Preparatory Commission on specific issues such as relations with the host Country and preparations for the First Session of the Conference of The States Parties (WHO, 2004).

The Preparatory Commission was successful in resolving a number of tasks within its mandate, the results of which were reflected in its Final Report. Among its major achievements were solutions to several substantive verification issues as well as the setting up of the OPCW Laboratory and Equipment Store, the development of a general training scheme for inspectors and the recruitment of inspector trainees, arrangements relating to the new OPCW headquarters building, and the development of draft documents such as the Headquarters Agreement, OPCW Staff and Financial Regulations, OPCW Health and Safety Policy and Regulations, OPCW Confidentiality Policy, and the OPCW Media and Public Affairs Policy. The Preparatory Commission was also responsible for the orderly transfer of its property, functions and recommendations to the OPCW. Despite its considerable efforts, however, the Preparatory Commission was unable to reach an agreement on a number of issues deriving from the Paris Resolution. These issues were therefore carried over to the OPCW as 'unresolved issues'. Many of these issues have been resolved since then, but others are still under discussion by the Member States of the OPCW (Thakur, 1999; Thakur & Ere, 2006).

Hungary was the 65th country to ratify the Convention, in late 1996, and on April 29, 1997, the CWC entered into force with 87 States Parties—becoming binding international law. An additional 22 countries had ratified the treaty in the 180 days between Hungary's ratification and entry into force. With the entry into force of the Convention, the OPCW immediately began its work to implement the Convention. Both, the Convention and its implementing body ,are intended to adapt not only to shifts in the international environment and the changing needs of State Parties, but also to respond to the rapid pace of scientific and technological developments. Every five years, the Convention foresees that the State Parties should undertake a review of the implementation process. These review conferences serve as fora for the assessment and evaluation of the CWC's implementation, and the identification of areas where change is needed. A particular focus is given to the verification regime and the changing context within which it is implemented as well as scientific and technological advances in chemistry, engineering and biotechnology. The first review conference was held from April 28 to May 9, 2003. The second review conference was held from April 7 to 18, 2008.

5. CONCLUSION

In conclusion, we can affirm that the use of chemical agents in history and present times has been a matter of several discussions and it resulted not only in the death of millions of people but also provoked new conflicts and huge historical events. The criticisms regarding the use of offensive chemical agents have also resulted in positive effects. The instauration of the CWC together with the born of the OPCW are two important milestones achieved by the international community that have improved the safety and security of people and the worldwide political and economical stability.

ACKNOWLEDGMENT

Special acknowledgement for the realisation of this work goes to the International Master Courses in Protection Against CBRNe Events (http://www.mastercbrn.com).

REFERENCES

Baldassi, F., D'Amico, F., Carestia, M., Cenciarelli, O., Mancinelli, S., Gilardi, F., Malizia, A., Di Giovanni, D., Soave, P.M., Bellecci, C., Gaudio, P. & Palombi, L. (2016). Testing the accuracy ratio of the Spatio-Temporal Epidemiological Modeler (STEM) through Ebola haemorrhagic fever outbreaks. *Epidemiol. Infect.*, In press.

Baudendistel, R. (1998). Force versus law: The International Committee of the Red Cross and chemical warfare in the Italo-Ethiopian war 1935–1936. *Int. Rev, Red Cross*, **38**: 81-104.

Bellecci, C., Gaudio, P., Gelfusa, M., Lo Feudo, T., Malizia, A., Richetta, M. & Ventura, P. (2009). Raman water vapour concentration measurements for reduction of false alarms in forest fire detection. *SPIE Rem. Sen.*, p. 74790H.

Cacciotti, I., Aspetti, P.C., Cenciarelli, O., Carestia, M., Di Giovanni, D., Malizia, A., D'Amico, F., Sassolini, A., Bellecci, C. & Gaudio, P. (2014). Simulation of Caesium-137 (^{137}Cs) local diffusion as a consequence of the Chernobyl accident using Hotspot. *Defence S&T Tech. Bull.,* 7:18-26.

Caldicott, D. (2002). The tools of the trade: Weapons of mass destruction. *Emerg. Med.*, **14**: 240-248.

Carestia, M., Pizzoferrato, R., Cenciarelli, O., D'Amico, F., Malizia, A., Gelfusa, M., Scarpellini, D. & P. Gaudio. (2014). Fluorescence measurements for the identification of biological agents features for the construction of a spectra database. *Fotonica AEIT Ital. Conf. Photon Technol. (Fotonica AEIT 2014)*, Naples, Italy, pp. 1-4.

Carestia, M., Pizzoferrato, R., Gelfusa, M., Cenciarelli, O., D'Amico, F., Malizia, A., Scarpellini, D., Murari, A., Vega, J. & Gaudio, P. (2014). Towards the implementation of a spectral data base for the detection of biological warfare agents. *SPIE Sec. Def.*, 92510I.

Carestia, M., Pizzoferrato, R., Gelfusa, M., Cenciarelli, O., Ludovici, G. M., Gabriele, J., Malizia, A., Murari, A., Vega, J. & Gaudio, P. (2015). Development of a rapid method for the automatic classification of biological agents' fluorescence spectral signatures. *Opt. Eng.*, **54**: 114105.

Cenciarelli, O. Pietropaoli, S, Frusteri, L., Malizia, A., Carestia, M., D'Amico, F., Sassolini, A., Di Giovanni, D., Tamburrini, A.,Palombi, L., Bellecci, C. & Gaudio, P. (2014). Biological emergency management: the case of Ebola 2014 and the air transportation involvement. *J. Microbial. Biochem. Tec.*, **6**:247-253.

Cenciarelli, O., Gabbarini, V., Pietropaoli, S., Malizia, A., Tamburrini, A., Ludovici, G.M., Carestia, M., Di Giovanni, D., Sassolini, A., Palombi, L., Bellecci, C. & Gaudio, P. (2015). Viral bioterrorism: Learning the lesson of Ebola virus in West Africa 2013–2015. *Virus Res.*, **210**: 318-326.

Cenciarelli, O., Pietropaoli, S., Malizia, A., Carestia, M., D'Amico, F., Sassolini, A., Di Giovanni, D., Rea, S., Gabbarini, V., Tamburrini, A., Palombi, L., Bellecci, C. & Gaudio, P. (2015). Ebola virus disease 2013-2014 outbreak in West Africa: An analysis of the epidemic spread and response. *Int. J. Microbiol.*, article ID 769121.

Ciparisse, J. F., Malizia, A., Poggi, L. A., Gelfusa, M., Murari, A., Mancini, A. & Gaudio, P. (2015). First 3D numerical simulations validated with experimental measurements during a LOVA reproduction inside the new facility STARDUST-Upgrade. *Fusion Eng. Des.*, **101**:204-208.

Gaudio P., Malizia A. & Lupelli, I. (2010). Experimental and numerical analysis of dust resuspension for supporting chemical and radiological risk assessment in a nuclear fusion device. *Proc. Int. Conf. Mat. Mod. Eng. Sci.*, **30**:2010-2030.

Gaudio, P., Gelfusa, M., Lupelli, I., Malizia, A., Moretti, A., Richetta, M., Serafini, C. & Bellecci, C. (2011). First open field measurements with a portable CO2 lidar/dial system for early forest fires detection. *SPIE Rem. Sen.,* p. 818213.

Gaudio, P., Gelfusa, M., Malizia, A., Parracino, S., Richetta, M., Murari, A. & Vega, J. (2014). Automatic localization of backscattering events due to particulate in urban areas. *SPIE Rem. Sen.,* p. 924413.

Gay, K. (2001). *Silent Death: The Threat of Chemical and Biological Terrorism*. Twenty-First Century Books, Minneapolis, Minnesota.

Gelfusa, M., Gaudio, P., Malizia, A., Murari, A., Vega, J., Richetta, M. & Gonzalez, S. (2014). UMEL: A new regression tool to identify measurement peaks in LIDAR/DIAL systems for environmental physics applications. *Rev. Sci. Instrum.*, **85**:063112.

Gelfusa, M.,, Malizia, A., Murari, A., Parracino, S., Lungaroni, M., Peluso, E. & Gaudio, P. (2015). First attempts at measuring widespread smoke with a mobile lidar system. *Fotonica AEIT Ital. Conf. Photon. Technol. (Fotonica AEIT 2015)*, Turin, Italy, pp. 1-4.

Lupelli, I., Gaudio, P., Gelfusa, M., Malizia, A., Belluzzo, I. & Richetta, M. (2014). Numerical study of air jet flow field during a loss of vacuum. *Fusion Eng. Des.*, **89**:2048-2052.

Malizia A., Quaranta, R. & Mugavero, R. (2010). CBRN Events in the subway system of Rome: Technical-managerial solutions for risk reduction. *Defence S&T Tech. Bull.*, **3**:140-157.

Malizia, A., Camplani, M., Gelfusa, M., Lupelli, I., Richetta, M., Antonelli, L., Conetta, F., Scarpellini, D., Carestia, M, Peluso, E., Gaudio, P., Salgado, L. & Bellecci, C. (2014). Dust tracking techniques applied to the STARDUST facility: First results. *Fusion Eng. Des.,* **89**: 2098-2102.

Malizia, A., Carestia, M., Cafarelli, C., Milanese, L., Pagannone, S., Pappalardo, A., Pedemonte, M., Latini, G., Barlascini, O., Fiorini, E., Soave, P.M., Di Giovanni, D., Cenciarelli, O., Antonelli, L., D'Amico, F., Palombi, L., Bellecci, C. & Gaudio, P. (2014). The free license codes as Decision Support System (DSS) for the emergency planning to simulate radioactive releases in case of accidents in the new generation energy plants. *WSEAS T. Environ. Dev.*, **10**:453-464.

Office of Technology Assessment (OTA) (1993). *Proliferation of Weapons of Mass Destruction: Assessment of Risks.* U.S. Congress, OTA-ISC-559, Washington DC.

Organization for the Prohibition of Chemical Weapons (OPCW) (1999). *The Chemical Weapons Convention – A Guided Tour of the Convention on the Prohibition of the Development, Production, Stockpiling and Use of Chemical Weapons and on Their Destruction*. Organization for the Prohibition of Chemical Weapons (OPCW), The Hague.

Organization for the Prohibition of Chemical Weapons (OPCW). (2016). *Genesis and Historical Development*. Organization for the Prohibition of Chemical Weapons (OPCW), The Hague.

Pazienza, M., Britti, M.S., Carestia, M., Cenciarelli, O., D'Amico, F., Malizia, A., Bellecci, C., Gaudio, P., Gucciardino, A., Bellino, M., Lancia, C., Tamburrini, A. & Fiorito, R. (2013). Application of real-time PCR to identify residual bio-decontamination of confined environments after hydrogen peroxide vaportreatment: Preliminary results. *J. Microb. Biochem. Technol.*, **6**:24-28.

Pazienza, M., Britti, M.S., Carestia, M., Cenciarelli, O., D'Amico, F., Malizia, A., Bellecci, C., Fiorito, R., Gucciardino, A., Bellino, M., Lancia, C., Tamburrini, A. & Gaudio, P. (2014).Use of particle counter system for the optimization of sampling, identification and decontamination procedures for biological aerosols dispersion in confined environment. *J. Microb. Biochem. Technol.*, **6**:43-48.

Raicevic, N. (2001). The history of prohibition of the use of chemical weapons in international humanitarian law. *Law Pol.*, **1**: 613-631.

Sassolini, A., Malizia, A., D'Amico, F., Carestia, M., Di Giovanni, D., Cenciarelli, O., Bellecci, C., Gaudio, P. (2014) Evaluation of the effectiveness of titanium dioxide (TiO_2) self-cleaning coating for increased protection against CBRN incidents in critical infrastructures. *Defence S&T Tech. Bull.,***7**:9-17.

Schindler, D. & Toman, J. (Eds.). (1973). *The Laws of Armed Conflicts: A Collection of Conventions, Resolutions, and Other Documents*. Brill, Geneva, Switzerland.

Stock, T., Haug, M., & Radler, P. (1996). Chemical and biological weapon developments and arms control*, SIPRI Yearbook*, pp. 661-708.

Stockholm International Peace Research Institute (SIPRI) (1971). *The Problem of Chemical and Biological Warfare, Vol. 1: The Rise of CB Weapons.* Humanity Press, New York.

Stockholm International Peace Research Institute (SIPRI) (1973). *The Problem of Chemical and Biological Warfare, Vol. 3: CBW and the Law of War.* Humanity Press, New York.

Thakur, R. (1999). Arms control, disarmament, and non-proliferation: A political perspective. *In* Jeffrey A. Larsen & Thomas D. Miller (Eds.), *Arms Control in the Asia-Pacific Region*. USAF Institute for National Security Studies, US Air Force Academy, Colorado Springs, pp. 39–61.

Thakur, R. & Ere. H. (2006). *The Chemical Weapon Convention: Implementation Challenges and Opportunities.* United Nations University Press, Hong Kong.

United Nation (UN) (1969). *Chemical and Bacteriological (Biological) Weapons and the Effects of Their Possible Use.* United Nation (UN), New York, USA.

World Health Organization (WHO) (2004). *Public Health Response to Biological and Chemical Weapons*. World Health Organization (WHO), Geneva, Switzerland.